nature microbiology

Article

https://doi.org/10.1038/s41564-025-02059-8

The food-associated resistome is shaped by processing and production environments

Received: 13 June 2024

Accepted: 11 June 2025

Published online: 30 July 2025

Check for updates

Narciso M. Quijada[1,2,3,17], José F. Cobo-Díaz[4,17], Vincenzo Valentino[5,17], Coral Barcenilla[4], Francesca De Filippis[5,6], Raul Cabrera-Rubio[7,8], Niccolò Carlino[9], Federica Pinto[9], Monika Dzieciol[2], Inés Calvete-Torre[10,11], Carlos Sabater[10,11], Francesco Rubino[12,13], Stephen Knobloch[14], Sigurlaug Skirnisdottir[14], Lorena Ruiz[10,11], Mercedes López[4], Miguel Prieto[4], Viggó Thór Marteinsson[14,15], Abelardo Margolles[10,11], Nicola Segata[9], Paul D. Cotter[7,16], Martin Wagner[1,2], Danilo Ercolini[5,6] & Avelino Alvarez-Ordóñez[4] ✉

Food production systems may act as transmission routes for antimicrobial-resistant (AMR) bacteria and AMR genes (AMRGs) to humans. However, the food resistome remains poorly characterized. Here 1,780 raw-material (milk, brine, fresh meat and so on), end-product (cheese, fish, meat products and vegetables) and surface (processing, cooling, smoking, ripening and packing rooms) samples from 113 food processing facilities were subjected to whole-metagenome sequencing. Assembly-free analyses demonstrated that >70% of all known AMRGs, including many predicted to confer resistance to critically important antibiotics, circulate throughout food production chains, with those conferring resistance to tetracyclines, β-lactams, aminoglycosides and macrolides being the most abundant overall. An assembly-based analysis highlighted that bacteria from the ESKAPEE group, together with *Staphylococcus equorum* and *Acinetobacter johnsonii*, were the main AMRG carriers. Further evaluation demonstrated that ~40% of the AMRGs were associated with mobile genetic elements, mainly plasmids. These findings will help guide the appropriate use of biocides and other antimicrobials in food production settings when designing efficient antimicrobial stewardship policies.

The rapid emergence and spread of antimicrobial (AM) resistance are among the most urgent threats to health, as many infections are becoming refractory to AM treatment[1]. It has been estimated that 4.95 million deaths were caused in 2019 by AM-resistant (AMR) micro-organisms[2], which places AMR as the third greatest cause of death globally[3], and it is estimated that these figures will increase if a global and coordinated action plan is not implemented[4,5].

The misuse of AMs, especially in clinical settings and by the society, but also in agriculture, farming and other agrifood-associated settings, has been identified as one of the major drivers of AMR increase[6]. In fact, an important share of the AM sold globally is used for farming[7]. However, despite the predicted high impact that the microbial content of foods may have on the human microbiome and health[8], the diversity of resistant bacteria and AMR genes (AMRGs) in food production systems remains poorly characterized, with the available studies focusing exclusively on certain pathogen–drug combinations[9,10].

Some micro-organisms are able to survive and persist in food processing environments, despite the cleaning and disinfection practices that take place routinely[11], and can serve as natural inoculants for foods[12]. While many environmental micro-organisms thriving in food

A full list of affiliations appears at the end of the paper. ✉e-mail: aalvo@unileon.es

processing plants play beneficial roles in food production, others can act as food spoilers and/or can pose a threat to human health, including through the transmission of AMRGs to the human gut microbiome[13,14]. However, the diversity of AMRGs circulating through processing environments from different food production sectors, and the impact on the resistome of end food products, is yet to be unravelled.

The possibilities offered by metagenomics for the in-depth characterization of microbial communities and their genomic content has created new opportunities to decipher resistomes and ascertain their risks, including their potential for mobilization[15]. The location of AMR determinants within mobile genetic elements (MGEs) represents a major concern, as MGE-mediated horizontal transfer facilitates AMRG spread[16]. This is especially true for plasmids, which have facilitated a tenfold increase in the carriage of AMR determinants from 2000 to 2020[17].

The hypothesis of this study is that a very diverse and sector-specific resistome circulates daily through food production settings and that the resistome of end food products is markedly shaped by production environments and the ecologic pressures imposed by processing. To test this hypothesis, 1,780 raw-material, end-product and surface samples from 113 food processing facilities were subjected to whole-metagenome sequencing by the MASTER EU Consortium (https://www.master-h2020.eu/), as summarized in Fig. 1. The analyses presented here provide an in-depth characterization of the occurrence of AMR determinants in foods and their processing environments, highlighting potential hotspots for their transfer and disclosing information on their carrier taxa and association with MGEs.

Results

Production surfaces show the highest AMRG load and diversity

Overall, 2.7 million sequences (0.006% of the total number of sequences) aligned to 528 different AMRG clusters, which corresponds to 72.8% of all known AMRG clusters in the ResFinder database. The occurrence differed widely among AMRG classes, from 55.6% for glycopeptides to 87.9% for amphenicols (Supplementary Table 1). Remarkably, only 20 AMRG clusters were considered as prevalent (that is, >0.1 counts per million reads (CPM) in >10% samples), representing 79.4% of all AMRG reads (Extended Data Fig. 1). The occurrence, diversity and richness of AMRGs were significantly higher in food contact surfaces (FCSs) and non-food contact surfaces (NFCSs) than in raw materials and/or end food products, with end products showing a higher AMRG load, in CPM, than raw materials (Fig. 2a). Regardless of sample type, AMRG loads and richness were significantly higher in meat production than in other production sectors (Extended Data Fig. 2a).

In a principal coordinates analysis based on between-sample dissimilarity (beta-diversity) in relative abundance of AMRG clusters according to the sample type, all comparisons (for meat, dairy, fish and vegetable production sectors) resulted in statistically significant differences (adonis *P* value of 0.001) (Fig. 2b). Significant differences in beta-diversity were also observed among industry categories for all sample types (Extended Data Fig. 2b).

AMRGs associated with resistance to tetracyclines, β-lactams and aminoglycosides dominated overall, although the patterns differed widely among industry and sample types (Fig. 2c). Tetracyclines AMRGs were particularly dominant in the meat industry and mainly in FCS (Fig. 2c and Extended Data Fig. 3). β-Lactam and aminoglycoside AMRGs were also abundant on meat processing surfaces, but not on food products or raw materials. In dairies, surfaces also showed the highest load of AMRGs, with β-lactam and aminoglycoside AMRGs being the most predominant, followed by tetracycline AMRGs, which were instead most prevalent in raw materials and final products (Fig. 2c). The lowest AMRG loads were found in fisheries, with near absence of AMRGs in raw materials and final products and with β-lactam and aminoglycoside AMRGs being dominant on surfaces (Fig. 2c). Finally, raw materials and FCSs contained the highest AMRG loads for vegetable factories, with notable variations in the resistome composition among sample types (β-lactam AMRGs were the most abundant on FCSs, while amphenicol, streptogramin and lincosamide AMRGs dominated in raw materials) (Fig. 2c). Interestingly, AMRGs from some AM families showed a higher occurrence in surfaces and final products (for example, macrolide AMRGs for all sectors; β-lactam AMRGs in facilities processing vegetables; fosfomycin AMRGs in meat production) and were almost absent in raw materials, suggesting that processing environments and not the input materials may act as the source of these AMRGs that contaminate the final products.

The most abundant AMRGs (>0.5 mean CPM per sample) found include various AMRGs of resistance to tetracyclines (*tet(S)* and *tet(M)*, mainly in dairy; *tet(L)*, *tet(K)* and *tet(39)*, mainly in meat) and aminoglycosides (*str*, *aph(6)-Id* and *aph(3″)-Ib*; mainly in dairy), together with some individual genes associated with resistance to either folate pathway antagonists, macrolides, fosfomycin, amphenicols or beta-lactams (for example, *sul2*, *fosD*, *mph(C)*, *oqxB*, *cmx*), and were in most cases more abundant on food processing surfaces than on raw materials and end products (Fig. 2d and Extended Data Fig. 1a).

A total of 665 different AMRGs, grouped in 121 gene clusters, associated with resistance to critically important antibiotics (CIAs), were detected in our study, which correspond to 69.5% and 72%, respectively, of all those included in the Resfinder database (Supplementary Table 1). Only *mph(C)* and *msr(A)* genes were within the most prevalent ARGs (Extended Data Fig. 1). Fish industries presented significantly lower CPM values for CIA-AMRGs than other industries (Extended Data Fig. 4a). Moreover, an increasing trend of CIA-AMRG abundance from raw materials to processing surfaces was observed in meat and dairy factories, with final products showing intermediate CPM values (Extended Data Fig. 4b). Among the CIA-AMRGs, *mph(C)*, *msr(E)*, *msr(A)*, *erm(B)*, *mecB*, *mecD* and *mph(E)* were the most abundant (>0.1 mean CPM per sample) and showed a differential distribution among sample and industry types (Extended Data Fig. 4c).

Diverse non-ESKAPEE taxa contribute to the food resistome

An assembly-based analysis rendered 8,584 contigs harbouring AMRGs from 1,152 samples. Among these, 5,446 contigs (63.4%) assigned to the species level were considered for downstream analysis. They were associated with 618 different species from 215 genera and were classified into 481 unique AMRGs (representing 19% of all AMRGs in Resfinder), associated with resistance against 18 different AM classes (Supplementary Table 1). β-Lactam AMRGs were those most frequently recovered (24.2% of all AMRGs), followed by aminoglycoside (20.8%), tetracycline (15.6%), amphenicol (12.5%) and macrolide (11.6%) AMRGs.

Staphylococcus, particularly the human-associated opportunistic pathogen *Staphylococcus aureus*, showed the greatest number of AMRG-carrying contigs (22.7% and 8.3%, respectively, of all AMRG-carrying contigs). This species belongs to the clinically relevant ESKAPEE group, which overall accounted for 18.9% of all AMRG-carrying contigs (Fig. 3 and Supplementary Table 2). Other ESKAPEE members, including *Acinetobacter baumannii* (2.3%), *Enterococcus faecium* (2.3%), *Escherichia coli* (2.3%), *Klebsiella pneumoniae* (1.4%) and *Pseudomonas aeruginosa* (1.1%), were also among the 20 main AMRG carriers. However, this indicates that the greatest contribution to the food resistome comes from non-ESKAPEE food-associated or commensal bacteria such as *Staphylococcus equorum* (6.6%), *Acinetobacter johnsonii* (5.9%), *Staphylococcus haemolyticus* (2.1%), *Staphylococcus saprophyticus* (1.7%), *Acinetobacter lwoffii* (1.7%), *Raoultella ornithinolytica* (1.5%) and *Brevibacterium zhoupengii* (1.5%) (Fig. 3 and Supplementary Table 2).

Some AMRGs were almost exclusively associated with certain taxa, such as *tetK*, *blaZ* and *ant(6)-Ia* with *S. aureus*, or *blaOXA-211*, *blaOXA-212*, *blaOXA-280* and *blaOXA-281* with *A. johnsonii*. Moreover, some micro-organisms with recognized positive effects in food production contributed with particular AMRGs, such as *S. equorum* carrying

https://doi.org/10.1038/s41564-025-02059-8

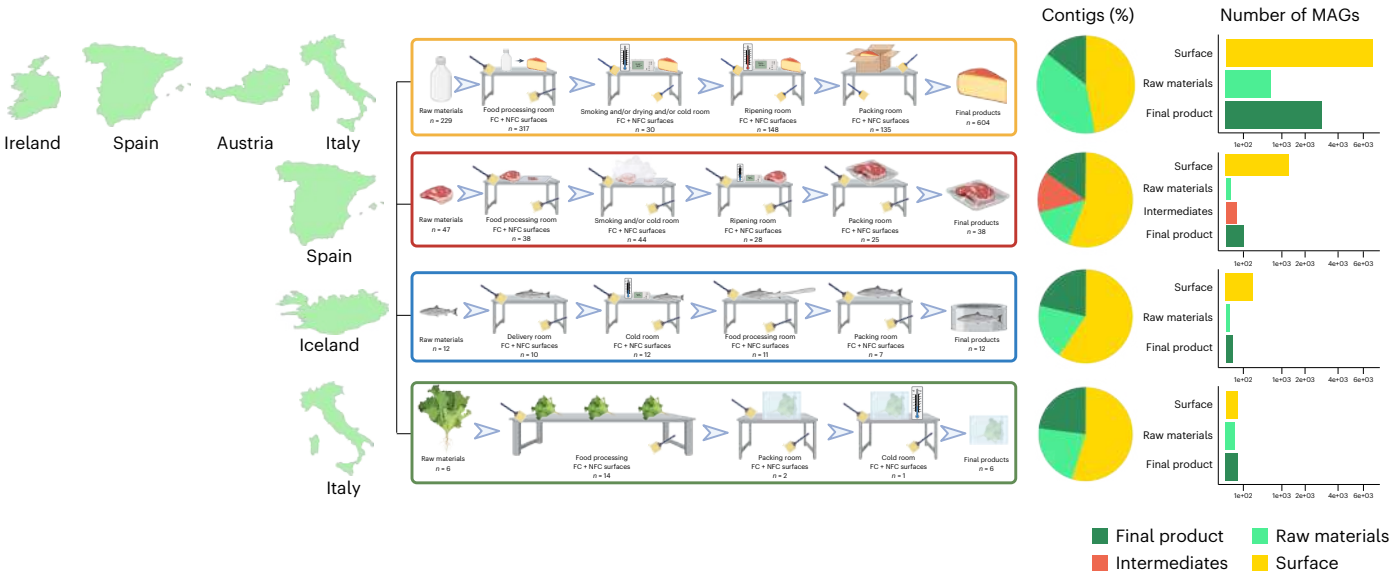

Fig. 1 | Sampling strategy and raw output of the metagenomic analysis. On the left side, countries of the visited industries are reported. For each industry type, the general process and sampling strategy is represented. The values indicate the total number of samples collected from raw materials, FCSs and NFCSs, and end food products. Also, for each industry type, pie and bar charts represent the proportion of contigs and the raw number of MAGs reconstructed from each sample type (that is, raw materials, final products, intermediate products and industry surfaces). Created with BioRender.com.

mph(C) and *fosD*, or *Brevibacterium aurantiacum* and *B. zhoupengii* carrying *cmx*, the most abundant AMRG in the study.

The distribution of AMRG-carrying species varied widely among production sectors and sample types (Fig. 3). Thus, while a wide range of species were identified as AMRG carriers in samples from dairy and meat production, the resistome of fish factories was mainly associated with *A. johnsonii* and that of vegetable facilities with *A. lwoffii* and *A. johnsonii*. Remarkably, considering the profile of AMRG-carrying taxa, in meat and dairy industries, processing surfaces and end products clustered together and separate from raw materials. This is explained by the relevance as carrier taxa exclusively in end products and production surfaces of *S. aureus*, *S. equorum*, *E. faecium*, *E. coli* and *K. pneumoniae* in meat production and *S. aureus*, *S. equorum*, *S. saprophyticus* and *B. zhoupengii* in dairy production.

The food resistome is highly linked to MGEs

The most abundant AMRGs identified by the assembly-based approach (those representing >2% of the total AMRGs), and their association with MGEs, are shown in Fig. 4. Overall, 31.7% of the AMRGs were identified to be plasmid associated, with 23% of them also presenting a plasmidic replicon (Supplementary Fig. 1). Other MGEs identified as harbouring AMRGs included unit transposons (Tns, 4.9%), insertion sequences (ISs, 4.0%), integrons (2.9%), miniature inverted repeats (MITEs, 0.7%), integrative conjugative elements (ICEs, 0.6%), composite transposons (ComTns, 0.2%) and integrative mobilizable elements (IMEs, 0.03%). Furthermore, WAAFLE[18] predicted the mobilization via potential lateral gene transfer (LGT) of 37 AMRGs (0.6%). Notably, when considering all these MGE types, 37.8% of all AMRGs were considered to be mobile owing to their association with a MGE (Supplementary Fig. 1a). The proportion of AMRGs contained in MGEs varied greatly among companies, rooms, surfaces and products, with meat and cheese final products and raw materials harbouring in general a higher ratio of AMRGs associated with MGEs (49.1% and 40.9% in meat and cheese products, respectively; Extended Data Fig. 5). It also differed widely among AM classes (Fig. 4a and Supplementary Fig. 1a) and ranged from 5.1% and 7.5% of AMRGs occurring in MGEs for fosfomycin and β-lactam resistance, respectively, to 65.8% and 71.0% for tetracycline and aminoglycoside resistance, respectively. Aminoglycoside resistance was mostly associated with plasmids (56.8%), Tns (17.3%), integrons (11.6%) and ISs (9.6%); tetracycline AMRGs were very frequently associated with plasmids (62.4%), ISs (4.0%) and ICEs (3.8%); and mobile β-lactam AMRGs were mainly associated with Tns (2.8%), MITEs (2.0%) and plasmids (1.6%) (Supplementary Fig. 1a).

The association of AMRGs with MGEs was particularly relevant for ESKAPEE bacteria, especially *E. coli* (84.8% of AMRGs associated with MGEs), *S. aureus* (68.1%) and *P. aeruginosa* (67.9%), mostly linked to plasmids (Fig. 4d). Interestingly, even though β-lactam AMRGs were generally not associated with MGE in the study, in *K. pneumoniae* 75% of them were associated with MGEs, mainly ComTns carrying *blaSHV-27*. Aminoglycoside AMRGs were highly associated with integrons, ISs and Tns in *A. baumannii*, *E. coli* and *P. aeruginosa* (Fig. 4d). Meanwhile, AMRGs carried by the most relevant non-ESKAPEE bacteria (for example, *S. equorum*, *A. johnsonii*, A. lwoffii, *R. ornithinolytica* and *B. zhoupengii*) were rarely associated with MGEs (Fig. 4d and Supplementary Fig. 1b), with some non-ESKAPEE *Staphylococcus*, including *S. haemolyticus* and *S. saprophyticus*, representing an exception, as they harboured their AMRGs mainly in plasmids (Supplementary Fig. 1b).

As a potential indication of AMRG transfer events, we analysed the AMRGs shared by different species in the same production facility by aligning the AMRGs and their surrounding regions with high confidence thresholds. We found a high occurrence of intergenera AMRG sharing in specific taxa pairs, such as *Jeotgalicoccus–Staphylococcus* (associated with β-lactam AMRGs), *Escherichia–Pseudomonas* and *Acinetobacter–Psychrobacter* (mainly associated with folate pathway antagonist AMRGs). (Extended Data Fig. 6). Eight of these AMRG sharing events involving large regions (harbouring >30 coding sequences (CDSs)) were found between *Corynebacterium* and *Rothia*. Shared regions carried mainly aminoglycoside, folate pathway antagonist, β-lactam, aminoglycoside, tetracycline and amphenicol AMRGs. Remarkably, they were harboured mainly in samples from processing surfaces and final products (Extended Data Fig. 6).

We also evaluated the potential of different AMRGs to be co-selected or transferred together by analysing their co-occurrence in the same contig in close proximity. In total, 18.1% of the AMRG-carrying

https://doi.org/10.1038/s41564-025-02059-8

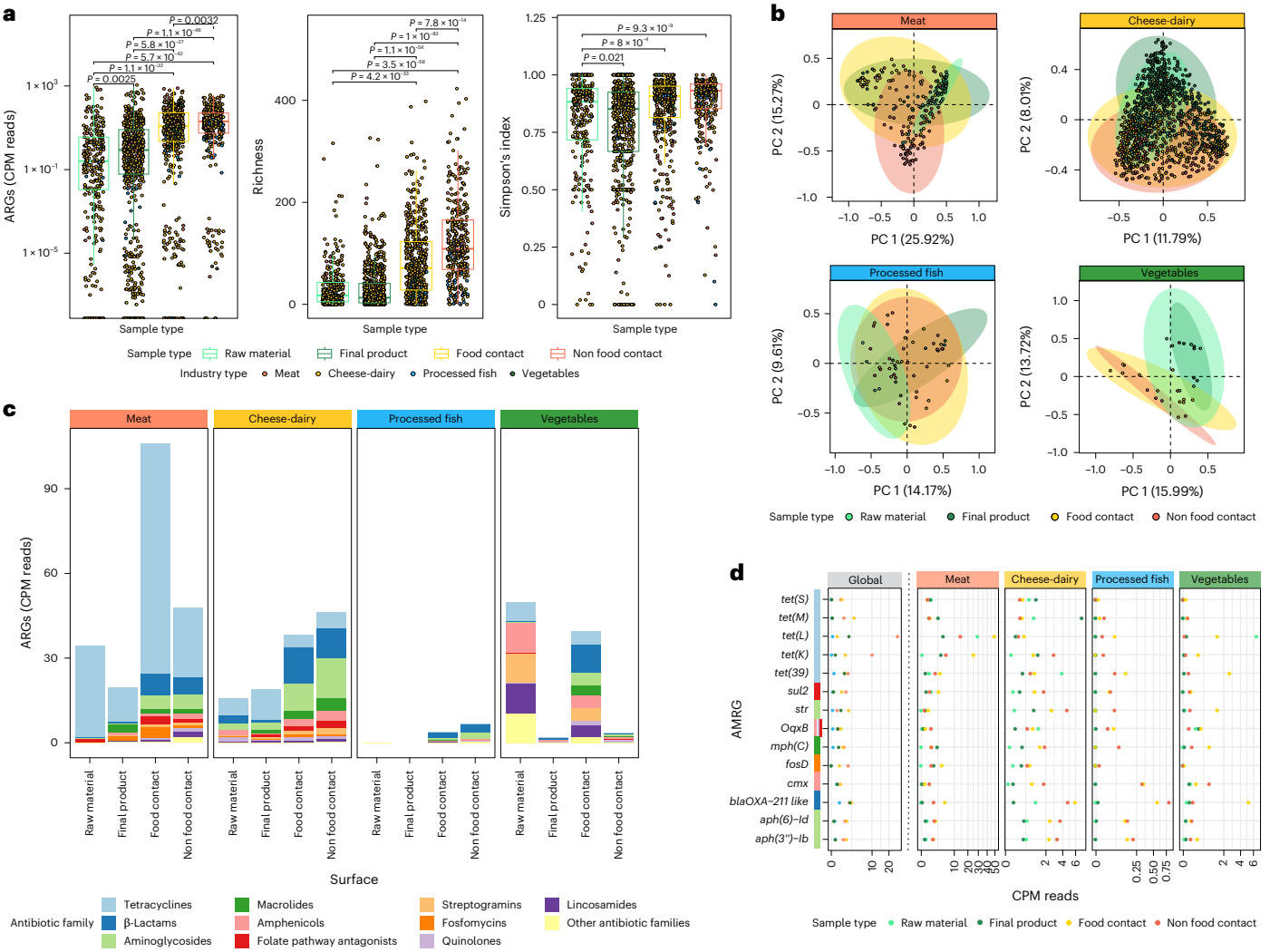

Fig. 2 | Quantitative overview of AMRG occurrence in foods and food processing environments. a, Total AMRG counts, richness index and Simpson's evenness index for AMRGs. *n* values were 294, 662, 489 and 335 for raw materials, final products, FCSs and NFCSs, respectively. The lower, middle and upper hinges in the box plots correspond to the first, second and third quartiles (the 25th, 50th or median and 75th percentiles), respectively. The upper whisker extends from the hinge to the largest value no further than 1.5× IQR from the hinge (where IQR is the interquartile range, or distance between the first and third quartiles). The lower whisker extends from the hinge to the smallest value at most 1.5× IQR of the hinge. Only significative *P* values (<0.05) are indicated according to the Wilcoxon test. **b**, Principal coordinates analysis for AMRG counts normalized to CPM. PC, principal coordinate. **c**, The relative abundance of AMRGs associated with the ten most abundant antibiotic families detected. For those genes conferring resistance to more than one antibiotic family, each antibiotic family was counted separately. AMRGs not included within the former ten most abundant families are represented as 'Other antibiotic families'. **d**, Average abundance of the main AMRG on each industry type and sample type, indicated by column and point colours, respectively, except for the first column, which shows a global comparative analysis among industry types. The coloured box next to each AMRG name corresponds to the antibiotic family the gene confers resistance to (*OqxB* is associated with resistance against three antibiotic families), according to the legend in the bottom left part of the figure. AMRG groups obtained at 90% identity clustering by CD-HIT were used for the analysis shown in this figure. *n* values for **b**–**d** are as follows: Meat – Raw material, 47; Final product, 38; Food contact, 67; Non food contact, 68. Cheese-dairy – Raw material, 229; Final product, 605; Food contact, 390; Non food contact, 240. Processsed fish – Raw material, 12; Final product, 13; Food contact, 20; Non food contact, 22. Vegetables – Raw material, 6; Final product, 6; Food contact, 12; Non food contact, 5.

contigs were identified to harbour two or more AMRGs. Among the most abundant patterns of co-occurrence, three involved CIA genes: *OqxA*–*OqxB*, found only on non-MGE contigs assigned to *Raoultella*, *Enterobacter*, *Lelliottia* and *Klebsiella* mainly from processing rooms; *mph(C)*–*msr(A)*, found only on plasmidic contigs, mainly from ripening and packing rooms, assigned to *Staphylococcus*; and *mph(E)*–*msr(E)*, found only on plasmidic contigs, mainly from processing rooms, assigned to *Acinetobacter and Klebsiella* (Fig. 5a). Some genes were largely found co-occurring with other AMRGs rather than as unique AMRGs in the contigs. These included *aph(3″)-Ib*, *aph(6)-Id*, *OqxA*, *OqxB*, *msr(A)*, *aadA2*, *mph(E)*, *msr(E)*, *aadA9*, *tet(G)* and *aph(3′)-III* (Fig. 5a). Except for the *OqxA*–*OqxB* and *aadA14*–*sul2* pairs, all the most prevalent co-occurrence gene patterns were mainly or entirely found in plasmid-related contigs, mainly in processing rooms and/or final products (Fig. 5a). The co-occurrence of AMRGs was primarily observed in ESKAPEE genera, *Psychrobacter*, *Raoultella* and *Moraxella* (Fig. 5a). Two AMRG patterns were found combined together in three final product samples from the same facility in a 26-kbp shared region that also contains seven genes related to mercury resistance and several regions associated with MGEs, as an integron containing *sul1*, *ant(3″)-Ia* and *dfrA1* (Fig. 5b). All AMRG patterns obtained have been found previously, mainly in plasmidic regions (except pattern 2 and pattern 10) (Supplementary Table 3).

https://doi.org/10.1038/s41564-025-02059-8

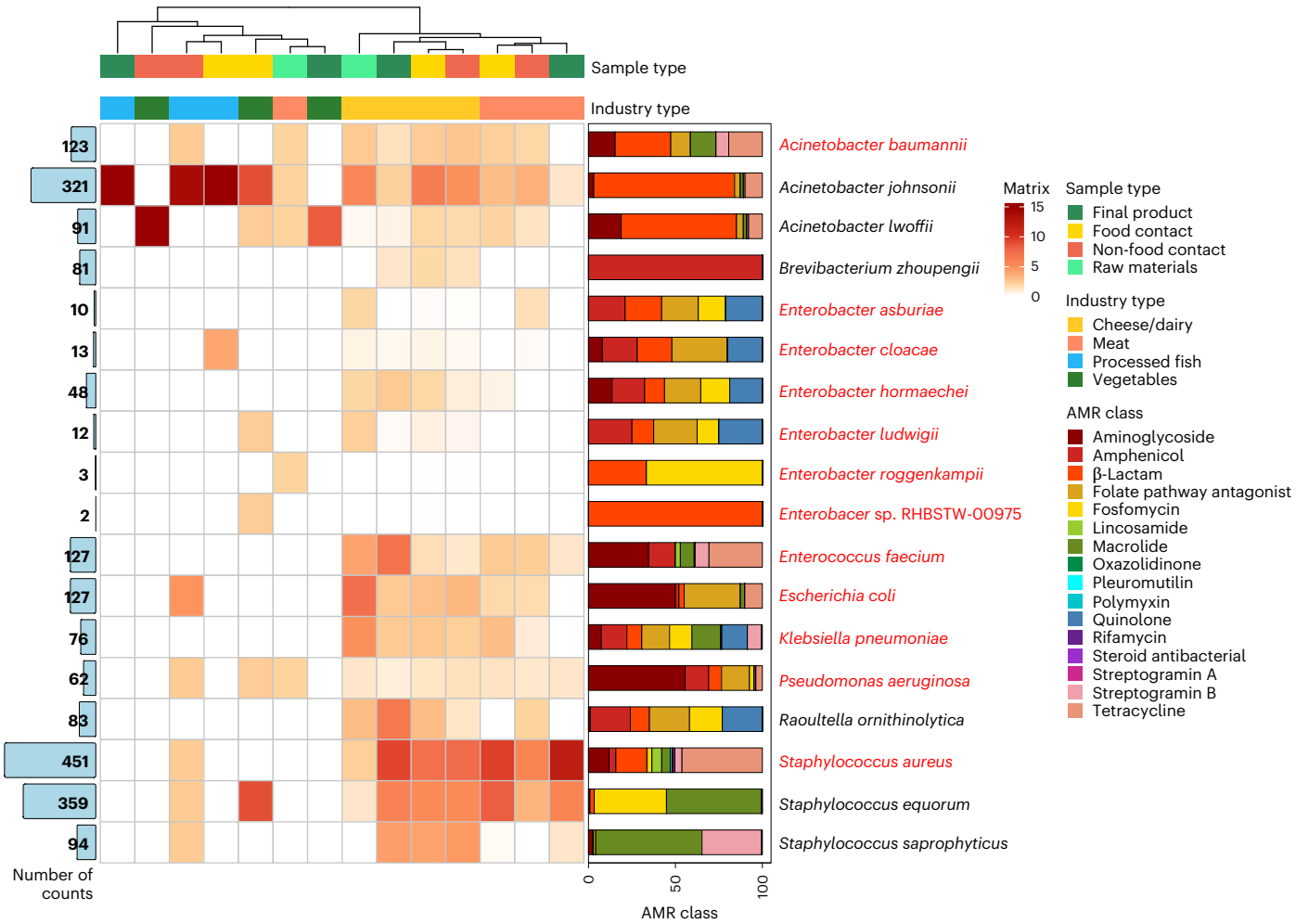

Fig. 3 | The most relevant AMRG-carrier bacterial species in the different food production sectors, with indication of their resistome profile. Heat map values were calculated by dividing the number of AMRG-encoding contigs (from each sample and industry type) assigned to the species indicated in the row by the total number of AMRG-encoding contigs (for the sample and industry type indicated in each column), to reduce overestimation in cheese and dairy industries due to unbalanced sampling. The left bar plot indicates the percentage of contigs assigned to each species on total number of AMRG-encoding contigs, while the right bar plot indicates the AMRG family distribution within each species, by percentage of total contigs. The most abundant species plus *Enterobacter* species, belonging to the ESKAPEE group, were plotted. Members of the ESKAPEE group are reported in red.

Meat and dairy contact surfaces are main sources of AMRGs in food

Meat production facilities were the most heterogeneous with respect to manufacturing procedures and nature of the final products (that is, fresh meat products, cured meats, aged meat and dry fermented sausages; Extended Data Fig. 7 and Supplementary Table 4). A comparison of the resistome profile of the different meat-production samples showed that raw materials clustered separately to all other sample categories, mainly due to the absence or very low occurrence of several AMRGs frequently found in surfaces and/or final products, such as *tet(K)*, *fosD*, *blaOXA-427*, *mph(C)*, *str*, *sul1* and *aadA1* (Fig. 6a). FCSs from ripening, smoking and cold rooms clustered with final products, mainly due to the high occurrence of *tet(K)* and *fosD* genes (Fig. 6a), assigned to *S. aureus* and *S. equorum*, respectively (Fig. 4). We further aimed to infer through contig alignment if some specific taxa were responsible for these AMRG-sharing events towards the final products and linked them mainly to *Acinetobacter* (originating from packing and ripening rooms, carrying *aph(6)-Id*), *Moraxella* (from ripening and cold rooms, carrying *addA14* and/or *sul2*), *Psychrobacter* (from packing rooms and raw materials, carrying *aph(6)-Id*) and *Staphylococcus* (present ubiquitously and carrying *tet(K)*) (Fig. 6c). To infer the potential origin of the AMRGs in the final meat products, we analysed the occurrence of the same AMRG variants in both the final products and other sources, on each individual facility, and represented it as a ratio of coincidence (Fig. 6e). It was observed that FCSs from the latest steps of production (that is, ripening and packing) harboured the greatest proportion of the AMRGs found in the final meat products.

In cheese production, cheese samples collected before ripening and raw materials clustered together and close to FCSs and NFCSs from processing and cold rooms, while final products clustered closer to samples from FCSs and NFCSs from later stages of production, including ripening and packing rooms (Fig. 6b). Remarkably, some AMRGs that were absent or rarely occurring on raw materials, the processing area or the freshly processed cheese showed a high occurrence in final products and industry surfaces. For example, *cmx* was assigned mainly to *Brevibacterium zhoupengii* (25.3% of all *cmx* genes), *Brevibacterium aurantiacum* (21.6%) and *Micrococcus luteus* (10.6%); *mph(C)* to *S. equorum* (65.9%) and *S. saprophyticus* (24.8%); *tetK* to *S. aureus* (93.8%); *fosD* to *Staphylococcus* species (96.0%), particularly *S. equorum* (67.8%); *blaZ* to *S. aureus* (46.2%), *Jeotgalicoccus* sp. (22.2%) and *Mammaliicoccus lentus* (19.9%); and *msrA* to *Staphylococcus* species (100%), particularly *S. saprophyticus* (89.1%). By contrast, other AMRGs were almost exclusively found in raw materials and end products, highlighting their persistence throughout cheese processing

https://doi.org/10.1038/s41564-025-02059-8

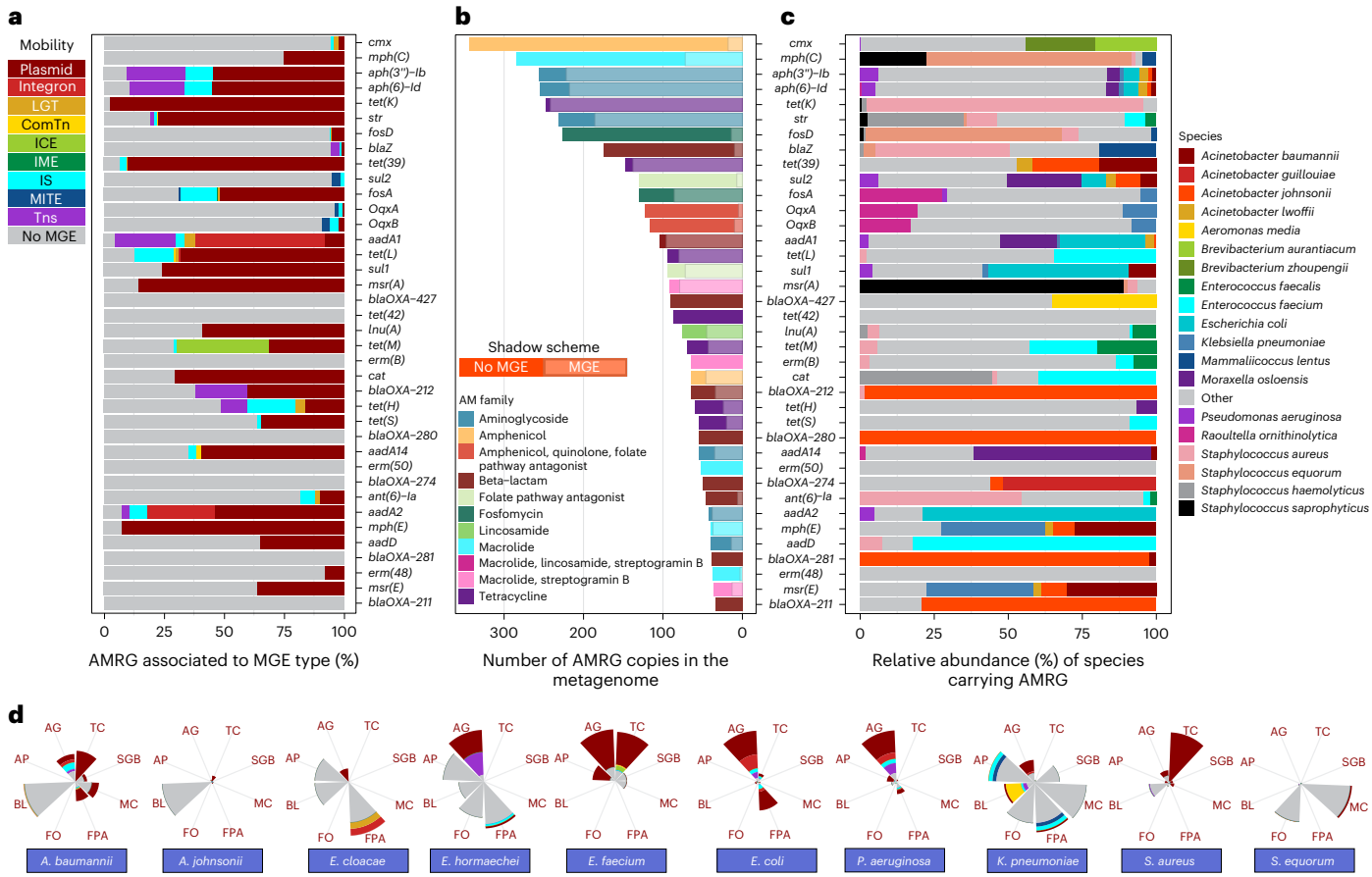

Fig. 4 | The most abundant AMRGs occurring in foods and food processing environments, with indication of their distribution across different taxa. **a**, The percentage of the most abundant AMRGs occurring in the different MGE types. **b**, The number of contigs harbouring the most abundant AMRGs found in the metagenomes analysed. Bars are coloured according to the AM families each AMRG confers resistance to. Shadow bars for each AMRG represent the number of those AMRGs that were identified to occur in any MGE. **c**, Taxonomic assignment of contigs carrying the most abundant AMRGs, expressed as relative abundance (% of contigs carrying the AMRG indicated on the *y* axis). **d**, The association of AMRGs with MGEs by AMRG class in ESKAPEE key taxa and other main AMRGs carrying taxa: *A. johnsonii* and *S. equorum*. The size of the pie graph portions indicates the number of AMRGs found for each AMRG class, while the colour indicates the proportion of AMRGs found associated with MGEs for the corresponding species and AMRG class, according to the legend shown on the bar plot figure. AG, aminoglycosides; AP, amphenicols; BL, β-lactams; FPA, folate pathway antagonists; FO, fosfomycin; MC, macrolides; TC, tetracyclines; SGB, streptogramin B.

and ripening, such as *tet(M)*, assigned mainly to *Lactococcus lactis* (22.6%), *Enterococcus faecalis* (22.6%) and *E. faecium* (21.0%); *tet(S)* to *Streptococcus parauberis* (63.8%); *erm(B)* to *Lactiplantibacillus plantarum* (22.6%), *Aerococcus urinaeequi* (14.5%) and *Staphylococcus pseudintermedius* (12.9%); and *ant(6)-Ia* to *S. aureus* (54.5%) (Fig. 3). A company-per-company analysis, performed as described above and shown in Fig. 6b, highlighted the role of both FCS and NFCS from the latest stages of cheese production (ripening and packing rooms) as the main source of AMRG-carrying bacteria in final products, while the influence was lower for the raw materials or the initial processing areas. AMRG spread events, identified through contig alignment, mainly involved *Staphylococcus* originating from ripening rooms (carrying *tet(K)*, *msr(A)*, *mph(C)*, *fosD*, *erm(C)* and/or *cat* genes), and *Acinetobacter* and *Streptococcus* originating mainly from processing rooms (carrying *tet(39)*, *sul2*, *blaOXA-373* and/or *tet(S)*) (Fig. 6d). Overall, FCSs from drying and ripening rooms showed a strong influence on the resistome of the final products (Fig. 6f).

More than 700 AMRG-carrying MAGs were reconstructed

Overall, 713 high-quality MAGs containing AMRGs were reconstructed. They were assigned to 85 known genera (mainly *Staphylococcus*, 13.5% of all AMRG-carrying MAGs; *Acinetobacter*, 10.4%; and *Raoultella*, 5.9%) and 264 different species (including 51 species not assigned to the genus level, coming from uncultured species genome bins), with *S. equorum*, *Acinetobacter guillouiae* and *Lactococcus lactis* being the most represented. MAGs from some species, such as *Raoultella ornithinolytica* and *Shewanella putrefaciens*, carried a very conserved resistome, while those from *S. equorum*, *A. guillouiae* and *L. lactis* had a more variable AMRG profile (Extended Data Fig. 8a). As could be expected, the number of different AMRGs and AMRG clusters found in MAGs was much lower than that found in contigs and in the assembly-free analysis (Extended Data Fig. 8b).

Discussion

This work provides a comprehensive survey of the resistome in foods and throughout the food production chain, based on a large number of samples collected (expanding the publicly available food-related metagenomes by ~3×), a wide diversity of food types and industrial surfaces sequenced, and a sequencing approach with increased depth (~2× depth, which yielded ~4× number of MAGs[19]). Detailed information was obtained on the main AMRGs occurring in food production systems, their possible association with specific taxa and MGEs and their spread across production sites. The application of whole-metagenome sequencing approaches in food industry settings faces important

https://doi.org/10.1038/s41564-025-02059-8

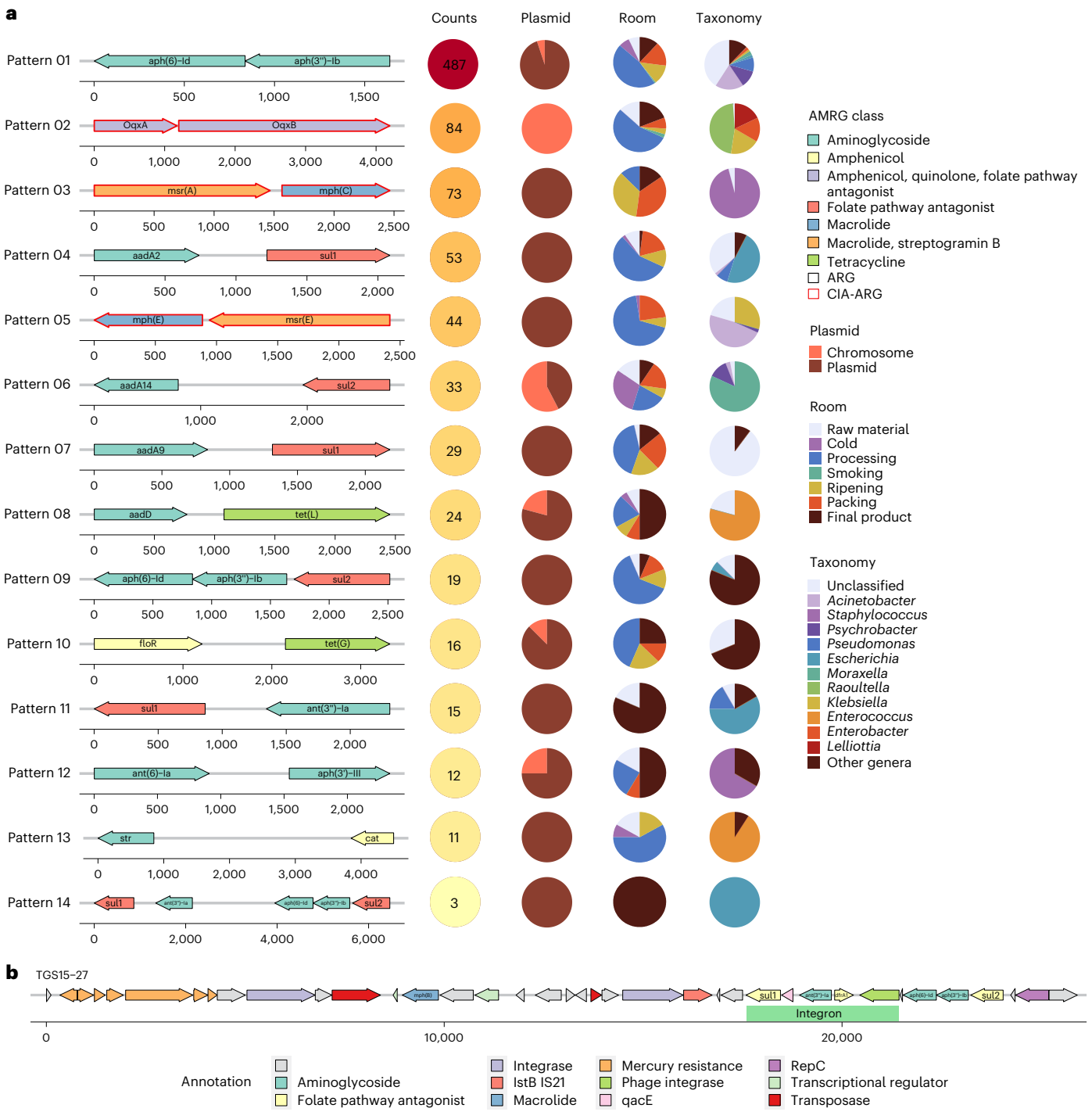

Fig. 5 | Co-occurrence of AMRGs within contigs. a, Circles indicate how often (%) the contigs carrying each co-occurrence pattern were assigned as plasmidic ('Plasmid' column); and the room and taxonomic assignment for the contigs ('Room' and 'Taxonomy' columns, respectively). Only those co-occurrence patterns with more than ten counts are indicated. AMRGs conferring resistance to CIAs are marked with red arrow lines. **b**, A gene location map representation of the *aph(3")-Ib-aph(6)-Id-sul2-ant(3")-Ia-sul1* pattern, found three times in contigs with identity >99.9% on the plotted region.

challenges, the most relevant one being the recovery of a sufficient amount of microbial DNA from the frequently low-biomass niches sampled. Another limitation is that sequences can originate from both dead and alive cells, although the detection of an AMRG still represents a potential risk for AMR spread[20]. In addition, the limited sensitivity of the technology for the detection of low-abundance micro-organisms might be overcome through the sequencing of enrichment cultures, although culturing steps introduce important biases in studies like ours focused on studying the biodiversity of systems as enrichments favour fast growers outcompeting other representative members of the community[21,22]. The MASTER EU Consortium has validated improved sampling and DNA extraction protocols for microbiome analysis tailored to food-processing environments[23]. Their application, combined with the bioinformatic tools and resources (cFMD and *foodGenVir* databases) described here and by Carlino et al.[19], and available in public repositories[24–26], greatly improves sequencing outcomes and will speed up the uptake of microbiome and resistome mapping approaches by the food research community and by industry stakeholders.

Our results indicate that the majority of known AMRGs (>70%), including many conferring resistance to CIAs, circulate daily throughout food production chains, although for most AMRGs the prevalence and abundance is overall low. We identified AMRGs associated with resistance to almost all known AM classes, with a higher representation of those linked to the AM classes most widely consumed in the European Union, that is, tetracyclines, β-lactams, aminoglycosides and macrolides[27]. While the results suggest that the resistome load and diversity is greater in the production of foods of terrestrial animal origin, in agreement with previous studies[28], this would require further confirmation, as our study was unbalanced towards a higher proportion of cheese and meat producers and was limited to a few European countries. Additional studies including more facilities from a wider range of food production sectors and countries would be highly beneficial, as countries have different policies regarding AM usage in agriculture and farming, which will probably be reflected in differences in resistome composition[29].

Some AMR ESKAPEE species are considered antibiotic-resistant priority pathogens posing the greatest threat to human health by the World Health Organization, prompting urgent calls for research into the development of new antibiotics effective against them[30]. We identified bacterial species belonging to the ESKAPEE group among the main carriers of AMRGs, mainly in cheese and meat factories and almost ubiquitously across all samples collected. Among them, *S. aureus*, a common member of the human skin microbiota that might appear in the processing environment through handling[31], was the most frequent AMRG carrier. However, other non-ESKAPEE micro-organisms that are frequently found in food production environments[32] and are not so well known or studied as carriers of AMRGs, such as *S. equorum*, *S. saprophyticus*, *A. johnsonii*, *A. lwoffii*, *R. ornithinolytica* or *B. zhoupengii*, were also identified as major contributors to the food production resistome. These findings should be the starting point for additional integrative initiatives specifically targeting these less known food-resistome-associated species aiming to better understand the risk they pose for AMR spread.

MGEs (mainly plasmids) play a crucial role in AMRG spread. As widely described before in other environments[17,33], a notable proportion (37.8%) of the AMRGs identified here in food production systems are potentially mobilizable. This was particularly relevant for some ESKAPEE species (*E. coli*, *P. aeruginosa* and *S. aureus*) and AM classes (aminoglycosides and tetracyclines), which thus pose the highest risk for the spread of AMR in food processing environments and to consumers. By contrast, most non-ESKAPEE species were rarely found carring MGE-associated AMRGs. For instance, *A. johnsonii*, a non-ESKAPEE bacterium associated with food spoilage and just occasionally described as an opportunistic pathogen[34], was widely distributed across foods and associated processing environments from all production sectors as a carrier of mainly chromosomal β-lactam *blaOXA*-type AMRGs; and various members of the genus *Staphylococcus* (*S. equorum* and *S. saprophyticus*) frequently found in food production environments[32] were abundant carriers of particular chromosomal AMRGs (*mph(C)* and *fosD* in *S. equorum* and *mph(C)* and *msr(A)* in *S. saprophyticus*), with low occurrence in raw materials and an enhanced representation in processing surfaces and final products.

Assigning taxonomy to contigs may have possible technical complications (especially if contigs are small or located within MGEs)[35] and could lead to wrong interpretations due to the overrepresentation in public repositories of genomic regions from certain taxa (for example, clinically associated ESKAPEE genomes). To avoid these issues, we have been conservative in our analyses, eliminating short contigs (<1,000 bp; <3 CDS) not taxonomically assigned at the species level. This strategy minimizes assignment errors and yields reliable taxonomic assignment of AMRG-carrying contigs with known affiliation with a marginal proportion of false taxonomic assignments almost exclusively involving plasmidic contigs that were erroneously assigned mainly to closely related taxa, as described in detail in the Methods. Overall, despite the potential limitations, we believe the approach followed here offers important benefits. It provides insights into the genetic background of AMRGs that cannot be obtained through an assembly-free analysis (due to the inability to assign AMRGs to carrier taxa or MGEs), or from analyses focused on MAGs, as only a small proportion of contigs are ultimately clustered into MAGs[36], making the reconstruction of MGEs particularly challenging[37].

We obtained solid evidence highlighting the impact that some manufacturing processes and processing environments have on the resistome of end products, which overall had a higher amount and richness of AMRGs than raw materials, including genes not present at all in the latter and possibly introduced later in the production chain. Important differences were observed in the resistome composition of foods between pre- and postripening stages of production, with end products showing AMRG profiles closely resembling those from surfaces from the latest stages of manufacture (ripening and packing rooms). Our findings contradict those of some previous studies reporting a decrease in the amount and diversity of AMRGs along slaughterhouse processing lines[38,39], suggesting that, although some processing procedures may be effective in reducing or containing the spread of resistant micro-organisms, new contamination events and other ecological forces along food processing lines may favour the introduction and/or expansion of other resistant micro-organisms and AMRGs. Overall, the facility surfaces and the microbial succession dynamics driven by processing conditions showed a greater impact on the resistome of end products than the raw inputs did. Factors such as temperature or humidity shifts, pH and water activity changes along fermentation and ripening, or frequency of cleaning and disinfection of surfaces, among others, can facilitate the expansion of specialized food-production-adapted AMR micro-organisms not present or present at very low abundance in raw materials, with good abilities to grow at low temperatures, pH and/or water activity, or to form biofilms in food production surfaces[40]. For instance, staphylococci, found here as main AMRG carriers in surfaces and end products, are well equipped to grow in products with intermediate or low water activity, such as fermented sausages or ripened cheeses[41,42]. Likewise, other main AMRG carriers, such as *Acinetobacter*, *Pseudomonas* or *Moraxella*, are frequently found in processing environments and are good

Fig. 6 | Spread of AMRGs across meat and dairy production sites and to end products. a,**b**, The relative abundance of the 50 most abundant AMRGs in meat (**a**) and dairy (**b**) facilities. The AM class of each gene is colour-indicated on the left part, while sample type and facility room are colour-indicated on top. The heat map colour scale indicates the number of AMRGs for each surface. The flow chart legend represents the flow that the food products (stars) follow from raw materials to final products along the food production system and the different rooms (trapezes). Swab samples were collected from surfaces (circles), coloured green if in contact with food products and purple if not. **c**,**d**, Resistome spread events between raw materials/processing environments and end products in meat (**c**) and dairy (**d**) producing facilities as revealed through the alignment analysis of AMRG-carrying contigs. The size of the boxes and lines are proportional to the number of spread events found. The right part of the figures corresponds to final product samples, where AMRG and genus are indicated. **e**,**f**, The percentage of the same AMRG variant found in the final products and other sample types from the same facility by using assembly-based approaches for meat (**e**) and dairy (**f**) producing facilities. Only those facilities where at least five AMRG variants were found in the final products were used for this analysis. The lower, middle and upper hinges in the box plots correspond to the first, second and third quartiles (the 25th, 50th or median and 75th percentiles), respectively. The upper whisker extends from the hinge to the largest value no further than 1.5× IQR from the hinge (where IQR is the interquartile range, or distance between the first and third quartiles). The lower whisker extends from the hinge to the smallest value at most 1.5× IQR of the hinge.

https://doi.org/10.1038/s41564-025-02059-8

biofilm formers, having representative species capable of growing at low temperatures[43].

The evaluation of potential AMRG spread events also showed linkages between the resistome of final products and that of surfaces, especially FCSs from ripening and packing rooms. Although this influence might be bidirectional, the fact that processing surfaces were sampled here before processing started, thus reflecting the resident microbiome, suggests they may serve as an important source of AMRGs in foods. Previous investigations have described the importance of the house-specific microbiome for the proper maturation of some food

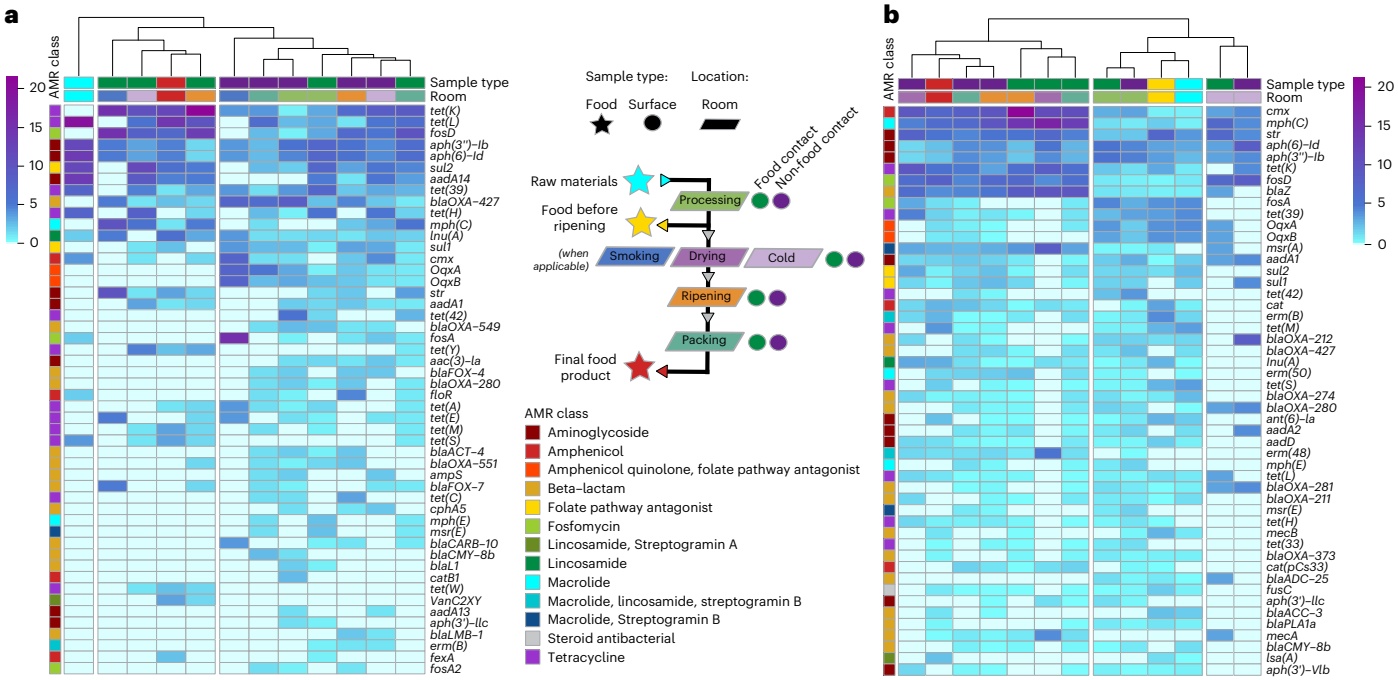

products and the development of their organoleptic properties[44]. Our results support the concept of 'natural contamination' of food products from the production environment[12], highlighting that processing plant microbiomes can greatly influence food safety by contributing to the spread of AMR bacteria that may cross-contaminate food products. Considering that industrial production of food relies on intense sanitation schemes to maintain a high level of hygiene as a means to ensure food quality and safety, and that some disinfectants and detergents used with this aim can impose selective pressures enhancing the chances of persistence of AMR micro-organisms and AMRG spread[45,46], our findings emphasize the importance of also considering the appropriate use of these agents in food production settings when designing efficient AM stewardship policies.

Methods

Sample collection, DNA extraction and sequencing

A total of 1,780 samples, taken from 113 food industries, were analysed in this study, including 824 from processing environments, 254 from raw materials and 702 final product samples (Supplementary Table 4). Samples from processing environments included FCSs (n = 489) and NFCSs (n = 335), which were sampled using Whirl-Pak Hydrated PolyProbe swabs (Whirl-Pak) to cover an area of about 1 m^2. Five swabs from each sample type (for example, floors and tables) were collected and pooled before DNA extraction. All the samples were stored at 4 °C and transported to the laboratory, where they were preprocessed within 24 h following the procedure described by Barcenilla et al.[23].

The surface of vegetables, fish, fresh meat and cured meat (both raw materials and end products) was also swabbed in sterile conditions, and five swabs per sample type were also pooled together and processed following the same procedures as for the environmental swabs.

Ten millilitres of phosphate-buffered saline (PBS) 1× were added to each pool of five swabs. After homogenization in the Stomacher (300 rpm × 30 s), the cell suspension was collected and aliquoted in 15-ml sterile tubes (Eppendorf), which were centrifuged at 14,000g for 2 min. Samples were washed twice with 2 ml of sterile PBS, and cell pellets were then stored at −80 °C until further processing for DNA purification.

Other types of samples collected included raw milk (50 ml), brine (when available, 200 ml), whey (200 ml), cheeses before ripening (2 cheeses) and after ripening (2 cheeses) in cheese industries; and meat batter (50 g), sausages before ripening (2 sausages) and after ripening (2 sausages) in factories producing dry fermented sausages. Raw milk and whey samples were centrifuged at 5,000g for 15 min at room temperature. The fat layer was carefully removed, and the supernatant was decanted. Cell pellets were resuspended with a sterile PBS solution, followed by a new centrifugation under the same conditions. This washing step was repeated once, and cell pellets were stored at −80 °C until further processing for DNA purification. Brine samples were prefiltered using 10-µm filters to remove large particles, and then the permeate was filtered through a 0.22-µm filter membrane. Micro-organisms were recovered from the 0.22-µm filter by placing the filter in a sterile 50-ml Falcon tube and adding 0.5 ml of sterile PBS, pipetting up and down for 1 min. Then, the suspension was centrifuged at 5,000g for 5 min at room temperature, and cell pellets were stored at −80 °C until further processing for DNA purification. For meat batter, cheese and sausage samples, 10 g were homogenized with 90 ml of PBS using a Stomacher at maximum speed for 2 min. Afterwards, the homogenate was centrifuged at 5,000g for 15 min at room temperature. Three serial washes with PBS were performed as described for milk and whey samples. Finally, cell pellets were stored at −80 °C.

DNA extraction was performed from the cellular pellets using a DNA extraction procedure recently developed for microbiome analysis in food processing environments, based on the PowerSoil Pro Kit of Qiagen with modifications, to increase total microbial DNA yields in low-biomass samples[23]. The DNA concentration was quantified using the Qubit HS Assay (Thermo Fisher Scientific).

Metagenomic libraries were prepared using the Nextera XT Index Kit v2 (Illumina), and whole-metagenome sequencing was performed on an Illumina NovaSeq platform using 150-bp PE, generating an average of 7.5 Gb and ~50 million PE reads per sample.

Raw sequencing data preprocessing

Reads were quality filtered and adapters were trimmed using a preprocessing pipeline[47], which includes TrimGalore[48] using --nextera--stringency 5--length 75--quality 20--max_n 2--trim-n parameters.

Assembly-free analysis

Filtered reads were aligned against the ResFinder database[49] (downloaded on 24 October 2022) using Bowtie2[50] with --very-sensitive--end-to-end parameters. Obtained sequence alignment map (SAM) files were filtered by an in-house ruby script[51], which removes the gene overestimation occurring when forward and reverse reads are aligned within the same gene. The obtained counts matrix was processed to calculate the CPM adding a 'bacterial marker' modification according to

$$\mathrm{CPM} = \frac{(\mathrm{AMRG} \times \mathrm{Bacterial\ marker\ alignments})}{\mathrm{Total\ number\ of\ reads}} \times 10^6,$$

where 'CPM' is the total CPM value for each AMRG and 'Bacterial marker alignments' is the value obtained from viromeQC[52], using --minlen 0--minqual 0 parameters, to normalize the dataset to consider only those reads derived from bacteria.

Reads are 150 bp in length and do not cover the entire length of the AMRG. As some AMRGs differ by just one or a few single-nucleotide polymorphisms, genes from the ResFinder database were clustered at 90% identity using CD-HIT[53] with default values to reduce the chance of the same read aligning to multiple closely related genes. The gene name used for each cluster obtained (gene cluster name), which was chosen according to the most abundant gene within each cluster or by the first number of the cluster within *bla* and *addA* genes, is indicated in the 'Genefam' column in Supplementary Table 3.

The AMRG richness and the Simpson diversity index values were calculated using the R package vegan[54] for alpha-diversity analysis, and statistical differences were evaluated with the Wilcoxon signed-rank test through the R package ggpubr[55]. Principal coordinates analyses with Bray–Curtis dissimilarities and Hellinger transformation using the vegdist function were used for beta-diversity analyses, and within-group dispersion was evaluated by the betadisper function. Both functions are located in the R package vegan[54]. Finally, the effects of industry type, surface and room on sample dissimilarities were determined by permutational multivariate analysis of variance using distance matrices (PERMANOVA) with the adonis function in the R package vegan[54]. The compare_means function in the R package ggpubr[55] was used to include statistically significant differences in the box plot figures.

In addition, the same alpha- and beta-diversity analyses were repeated on a subset of AMRGs conferring resistance to CIAs, selected according to previous publications[56–58].

Assembly-based analysis

For each sample, high-quality reads were assembled by using Megahit v1.1.1[59]. Contigs' files were imported into the TORMES v1.3.0 pipeline[60] (parameters: --min_contig_len 1000--only_gene_prediction--prodigal_options '-p meta' --gene_min_id 80--gene_min_cov 80), which discards contigs below 1,000 bp in length. The taxonomy of the remaining contigs was assigned using Kraken2[61] and the k2_pluspfp_20221209 database, and predicted and translated CDSs and proteins were extracted using Prodigal[62]. The screening of AMRGs in contigs was performed using BLASTN[63], integrated in ABRicate (Seemann[64]), against the ResFinder database[49] (downloaded on 24 October 2022). The output file

was manually curated to solve BLASTN and ABRicate issues associated with their default option 'culling_limit = 1', which wrongly annotated the variants of the aminoglycosides resistance genes *aadA* as *ant(3″)-Ia*, even when the identity and the coverage of the latter was lower. Contigs with a length below 1,000 bp and fewer than 3 CDSs per contig (26.1% of the total number of contigs) were discarded. The thresholds were decided after thorough evaluation of the methodology being applied over (1) mock communities used as positive controls (ZymoBIOMICS Microbial Community Standard D6300; Zymo Research) in three different concentrations (that is, 10^{-2}, 10^{-4} and 10^{-6}) and in four different laboratories; (2) 4,229 genomes (belonging to the most abundant AMRG-carrying species found in this study, that is, *A. baumannii*, *A. johnsonii*, *E. faecium*, *E. coli*, *S. aureus* and *S. equorum*) downloaded from RefSeq; (3) assessing the confidence and root-to-leaf (RTL) scores provided by Kraken2 (after polishing confidence values with Conifer v1.0.2[65]) accounting to taxonomic assignment per ranks and contig lengths; and (4) benchmarking compared with SqueezeMeta pipeline[66]. The methodology and results are thoroughly described and discussed in the Supplementary Information. Only the contigs assigned to the species level were considered for the downstream resistome and mobilome analysis. When possible, pipelines were parallelized to optimize computing resources by using GNU-Parallel[67].

The potential presence of AMRGs in MGEs was evaluated by using different software and in-house scripts. The evaluation of plasmids was performed directly over the AMRG-carrying contigs by using Platon v1.6[68] and by enabling the option --meta and geNomad v1.6.1[69]. In addition, the AMRG-carrying contigs were screened for the presence of plasmid replicons using the PlasmidFinder database[70] and the BLASTN and ABRicate commands implemented in TORMES. Contigs were considered to be plasmidic when a plasmid replicon was present and/or when both Platon (enabling --meta option) and geNomad (enabling end-to-end option) detected a contig to be plasmidic. The occurrence of integrons was evaluated using IntegronFinder v2.0.1[71]. Potential LGT events were evaluated using WAAFLE v1.0.0[18]. The location of AMRGs within integron regions was confirmed using the 'ARG-contig_mobilome_analysis' pipeline[72]. MobileElementFinder v1.0.5[73] was used to screen AMRG-carrying contigs for the detection of MITEs, ISs, ComTns, Tns, ICEs, IMEs and *cis*-mobilizable elements (setting flag --min-coverage 0.8).

Finally, an approach developed by Groussin et al.[74] was used for AMRG sharing events. AMRG-carrying contigs were aligned with themselves by BLASTN using 99.9% identity and 500-bp alignment length cut-offs, and aligned regions were extracted to confirm the presence of AMRGs by BLASTN against the Resfinder database using 80% identity and subject coverage cut-offs. Only those hits between two different samples from the same food processing facility were kept for further analysis of AMRG spread events (when query and subject sequences were assigned to the same genus) and genera AMRG sharing events (when query and subject sequences were assigned to different genera). The functional annotation of shared regions was performed by eggnog-mapper v2.1.11[75] using MMseqs2[76] with eggNOG DB v5.0.2. Output files from eggnog-mapper were transformed using an in-house script[77] into a gggenes formatted table, which was manually curated to then perform gene distribution plots by using the gggenes R package[78]. In addition, those contigs of particular interest (that is, carrying multiple AMRGs and/or MGEs) were aligned with BLASTN against the nt database[79] to assess whether such contig structures had been previously found.

The reconstruction of metagenome-assembled genomes (MAGs) was performed as described by Carlino et al.[19]. In brief, high-quality reads from each sample were mapped to their corresponding assembled contigs by using bowtie2 v2.2.9[80], and by enabling parameters '--very-sensitive-local' and '--no-unal'. Then, the jgi_summarize_bam_contig_depths script from MetaBAT v2.12.1[81] was used to calculate contig depth values from the SAM files obtained after bowtie2 alignment, as a preliminary step before contig binning with MetaBAT2. Only contigs longer than 1,500 bp were subjected to binning. The CheckM v1.0.13 'lineage_wf' workflow[82] was used to assess the quality of putative reconstructed genomes, and only those with completeness ≥50% and contamination < 5% (that is, medium- and high-quality MAGs, with high-quality MAGs being those with completeness >90% (ref. 83) were retained for further analyses. Average nucleotide identity among quality-controlled genomes was computed through Mash[84]. MAGs were then imported into the TORMES v1.3.0 pipeline[60] for CDS prediction, annotation and resistome evaluation by using the same parameters described above for the contigs dataset.

The MAGs containing AMRGs were used to create the foodGenVir database, a database containing AMRG-carrying MAGs from food and food-related environments that is publicly available via Zenodo at ref. 85, together with information on their origin and AMR profile, among other information. It is important to acknowledge that many AMR determinants associated with MGEs may not be represented in the database, as non-chromosomally encoded contigs are normally not clustered into MAGs during binning.

Data visualization

Statistic analyses and data handling towards visualization were performed under R environment v4.3.1[86], by using circlize v0.4.16[87], ComplexHeatmap v2.22.0[88], dplyr v1.1.4[89], ggalluvial v0,12.5[90], gggenes v0.5.1[78], ggplot2 v3.5.1[91], ggpubr v0.6.0[55], ggtree v3.14.0[92], khroma v1.16.0[93], pheatmap v1.0.12[94], reshape2 v1.4.4[95], tidyr v1.3.1[96] and vegan v2.6.10[54] packages. Antibiotic families from the ResFinder database were reorganized to facilitate and simplify data visualization. Only one-type antibiotic families were kept, and CPMs for each of these one-type antibiotic families were calculated by adding up the CPMs found on every ResFinder-Antibiotic family containing the one-type antibiotic family. As an example, the 'Oxazolidinone' family also contains those genes attached to the 'Amphenicol, Oxazolidinone, Tetracycline', 'Oxazolidinone, Amphenicol' and 'Oxazolidinone, Amphenicol, Lincosamide, Streptogramin A, Pleuromutilin' families from ResFinder.

Reporting summary

Further information on research design is available in the Nature Portfolio Reporting Summary linked to this article.

Data availability

Raw reads are available on the Sequence Read Archive of the National Center of Biotechnology Information (NCBI) under the BioProject numbers PRJNA897099 for vegetable facilities, PRJNA997800 for meat facilities and PRJNA997821 for cheese facilities, except those located in Ireland. Raw reads for fish processing factories and Irish cheese factories are available on the European Nucleotide Archive database under accession numbers PRJEB62794 and PRJEB63604, respectively. The specific BioSample, BioProject and public accession IDs for each sample, together with additional metadata are provided in Supplementary Table 4. The FoodGenVir database is publicly available via Zenodo at https://doi.org/10.5281/zenodo.8344969 (ref. 85).

Code availability

The pipelines and scripts used for reads filtering, assembly and binning, and resistome analysis are available via GitHub at https://github.com/SegataLab/MASTER-WP5-pipelines/tree/master/02-Preprocessing, https://github.com/SegataLab/MASTER-WP5-pipelines/tree/master/05-Assembly_pipeline, and https://github.com/nmquijada/MASTER-food-production-resistome, respectively.

References

1. Fisher, M. C., Hawkins, N. J., Sanglard, D. & Gurr, S. J. Worldwide emergence of resistance to antifungal drugs challenges human health and food security. *Science* **360**, 739–742 (2018).

2. Antimicrobial Resistance Collaborators. Global burden of bacterial antimicrobial resistance in 2019: a systematic analysis. *Lancet* **399**, 629–655 (2022).
3. GBD 2019 Diseases and Injuries Collaborators. Global burden of 369 diseases and injuries in 204 countries and territories, 1990-2019: a systematic analysis for the Global Burden of Disease Study 2019. *Lancet* **396**, 1204–1222 (2020).
4. O'Neill, J. I. M. *Antimicrobial resistance: tackling a crisis for the health and wealth of nations.* (The Review on Antimicrobial Resistance, 2014); https://amr-review.org/sites/default/files/AMR%20Review%20Paper%20-%20Tackling%20a%20crisis%20for%20the%20health%20and%20wealth%20of%20nations_1.pdf
5. *WHO: Antimicrobial Resistance, 2023* (WHO, 2024).
6. Kumar, A. & Pal, D. Antibiotic resistance and wastewater: correlation, impact and critical human health challenges. *J. Environ. Chem. Eng.* **6**, 52–58 (2018).
7. Van Boeckel, T. P. et al. Reducing antimicrobial use in food animals. *Science* **357**, 1350–1352 (2017).
8. Singh, R. K. et al. Influence of diet on the gut microbiome and implications for human health. *J. Transl. Med.* **15**, 73 (2017).
9. Temkin, E. et al. Estimating the number of infections caused by antibiotic-resistant *Escherichia coli* and *Klebsiella pneumoniae* in 2014: a modelling study. *Lancet Glob. Health* **6**, e969–e979 (2018).
10. O'Neill, J. *Tackling drug-resistant infections globally: final report and recommendations.* (The Review on Antimicrobial Resistance, 2016); https://amr-review.org/sites/default/files/160518_Final%20paper_with%20cover.pdf
11. Buchanan, R. L., Gorris, L. G. M., Hayman, M. M., Jackson, T. C. & Whiting, R. C. A review of *Listeria monocytogenes*: an update on outbreaks, virulence, dose-response, ecology, and risk assessments. *Food Control* **75**, 1–13 (2017).
12. Quijada, N. M. et al. Autochthonous facility-specific microbiota dominates washed-rind Austrian hard cheese surfaces and its production environment. *Int. J. Food Microbiol.* **267**, 54–61 (2018).
13. De Filippis, F., La Storia, A., Villani, F. & Ercolini, D. Exploring the sources of bacterial spoilers in beefsteaks by culture-independent high-throughput sequencing. *PLoS ONE* **8**, e70222 (2013).
14. Mulani, M. S., Kamble, E. E., Kumkar, S. N., Tawre, M. S. & Pardesi, K. R. Emerging strategies to combat ESKAPE pathogens in the era of antimicrobial resistance: a review. *Front. Microbiol.* **10**, 539 (2019).
15. Quijada, N. M., Hernández, M. & Rodríguez-Lázaro, D. High-throughput sequencing and food microbiology. *Adv. Food Nutr. Res.* **91**, 275–300 (2020).
16. Peterson, E. & Kaur, P. Antibiotic resistance mechanisms in bacteria: relationships between resistance determinants of antibiotic producers, environmental bacteria, and clinical pathogens. *Front. Microbiol.* **9**, 2928 (2018).
17. Wang, X. et al. Global increase of antibiotic resistance genes in conjugative plasmids. *Microbiol. Spectr.* **11**, e0447822 (2023).
18. Hsu, T. Y. et al. Profiling lateral gene transfer events in the human microbiome using WAAFLE. *Nat. Microbiol.* **10**, 94–111 (2025).
19. Carlino, N. et al. Analysis of 2,500 food metagenomes reveals unexplored microbial diversity and links with the human microbiome. *Cell* **187**, 5775–5795 (2024).
20. Pires, S. M., Duarte, A. S. & Hald, T. Source attribution and risk assessment of antimicrobial resistance. *Microbiol. Spectr.* **6**, 3 (2018).
21. McHugh, A. J. et al. Microbiome-based environmental monitoring of a dairy processing facility highlights the challenges associated with low microbial-load samples. *npj Sci. Food* **5**, 4 (2021).
22. Prakash, O., Parmar, M., Vaijanapurkar, M., Rale, V. & Shouche, Y. S. Recent trend, biases and limitations of cultivation-based diversity studies of microbes. *FEMS Microbiol. Lett.* **368**, fnab118 (2021).
23. Barcenilla, C. et al. Improved sampling and DNA extraction procedures for microbiome analysis in food-processing environments. *Nat. Protoc.* **19**, 1291–1310 (2024).
24. Segata, N. cFMD. *GitHub* https://github.com/SegataLab/cFMD (2025).
25. Segata, N. MASTER-WP5-pipelines. *GitHub* https://github.com/SegataLab/MASTER-WP5-pipelines (2024).
26. Quijada, N.M. MASTER-food-production-resistome. *GitHub* https://github.com/nmquijada/MASTER-food-production-resistome (2025).
27. *Antimicrobial Resistance in the EU/EEA—A One Health Response* (ECDC, 2022).
28. Munk, P. et al. The European livestock resistome. *mSystems* **9**, e0132823 (2024).
29. Zhao, C., Wang, Y., Mulchandani, R. & Van Boeckel, T. P. Global surveillance of antimicrobial resistance in food animals using priority drugs maps. *Nat. Commun.* **15**, 763 (2024).
30. Summary for policymakers. In *Intergovernmental Panel on Climate Change – Climate Change 2013 – The Physical Science Basis* (ed. IMO) 1–30 (Cambridge Univ. Press, 2014); https://doi.org/10.1017/CBO9781107415324.004
31. Krismer, B., Weidenmaier, C., Zipperer, A. & Peschel, A. The commensal lifestyle of *Staphylococcus aureus* and its interactions with the nasal microbiota. *Nat. Rev. Microbiol.* **15**, 675–687 (2017).
32. Marino, M., Frigo, F., Bartolomeoli, I. & Maifreni, M. Safety-related properties of staphylococci isolated from food and food environments. *J. Appl. Microbiol.* **110**, 550–561 (2011).
33. Goren, M. G. et al. Transfer of carbapenem-resistant plasmid from *Klebsiella pneumoniae* ST258 to *Escherichia coli* in patient. *Emerg. Infect. Dis.* **16**, 1014–1017 (2010).
34. Kämpfer, P. in *Encyclopedia of Food Microbiology* (eds Batt, C. A. & Tortorello, M. L.) 11–17 (Elsevier, 2014); https://doi.org/10.1016/B978-0-12-384730-0.00002-1
35. Fishbein, S. R. S., Mahmud, B. & Dantas, G. Antibiotic perturbations to the gut microbiome. *Nat. Rev. Microbiol.* **21**, 772–788 (2023).
36. Maguire, F. et al. Metagenome-assembled genome binning methods with short reads disproportionately fail for plasmids and genomic Islands. *Microb. Genom.* **6**, mgen000436 (2020).
37. Brown, C. L. et al. Critical evaluation of short, long, and hybrid assembly for contextual analysis of antibiotic resistance genes in complex environmental metagenomes. *Sci. Rep.* **11**, 3753 (2021).
38. Li, L. et al. Exploring the resistome, virulome, mobilome and microbiome along pork production chain using metagenomics. *Int. J. Food Microbiol.* **371**, 109674 (2022).
39. Campos Calero, G. et al. Deciphering resistome and virulome diversity in a porcine slaughterhouse and pork products through its production chain. *Front. Microbiol.* **9**, 2099 (2018).
40. Li, S. et al. Microbiome-informed food safety and quality: longitudinal consistency and cross-sectional distinctiveness of retail chicken breast microbiomes. *mSystems* **5**, e00589–20 (2020).
41. Li, H., Zhu, Q., Chen, X., Zhou, J. & Wu, J. Isolation and characterization of coagulase negative staphylococci with high proteolytic activity from dry fermented sausages as a potential starter culture. *Food Res. Int.* **162**, 111957 (2022).
42. Klempt, M., Franz, C. M. A. P. & Hammer, P. Characterization of coagulase-negative staphylococci and macrococci isolated from cheese in Germany. *J. Dairy Sci.* **105**, 7951–7958 (2022).
43. Møretrø, T. & Langsrud, S. Residential bacteria on surfaces in the food industry and their implications for food safety and quality. *Compr. Rev. Food Sci. Food Saf.* **16**, 1022–1041 (2017).
44. Bokulich, N. A. & Mills, D. A. Facility-specific "house" microbiome drives microbial landscapes of artisan cheesemaking plants. *Appl. Environ. Microbiol.* **79**, 5214–5223 (2013).

45. Botelho, J., Cazares, A. & Schulenburg, H. The ESKAPE mobilome contributes to the spread of antimicrobial resistance and CRISPR-mediated conflict between mobile genetic elements. *Nucleic Acids Res.* **51**, 236–252 (2023).
46. Palleja, A. et al. Recovery of gut microbiota of healthy adults following antibiotic exposure. *Nat. Microbiol.* **3**, 1255–1265 (2018).
47. Segata, N. MASTER-WP5-pipelines. *GitHub* https://github.com/SegataLab/MASTER-WP5-pipelines/tree/master/02-Preprocessing (2024).
48. Krueger, F. TrimGalore. *GitHub* https://github.com/FelixKrueger/TrimGalore (2023).
49. Zankari, E. et al. Identification of acquired antimicrobial resistance genes. *J. Antimicrob. Chemother.* **67**, 2640–2644 (2012).
50. Langmead, B., Wilks, C., Antonescu, V. & Charles, R. Scaling read aligners to hundreds of threads on general-purpose processors. *Bioinformatics* **35**, 421–432 (2019).
51. Segata, N. MASTER-WP5-pipelines. *GitHub* https://github.com/SegataLab/MASTER-WP5-pipelines/blob/master/07-AMR_virulence_genes/count_reads.rb (2024).
52. Zolfo, M. et al. Detecting contamination in viromes using ViromeQC. *Nat. Biotechnol.* **37**, 1408–1412 (2019).
53. Fu, L., Niu, B., Zhu, Z., Wu, S. & Li, W. CD-HIT: accelerated for clustering the next-generation sequencing data. *Bioinformatics* **28**, 3150–3152 (2012).
54. Oksanen, J. et al. vegan: Community Ecology Package. R version 4.3.1 (2022).
55. Kassambara, A. ggpubr: "ggplot2" Based Publication Ready Plots. R version 4.3.1 (2023).
56. Cobo-Díaz, J. F. et al. Microbial colonization and resistome dynamics in food processing environments of a newly opened pork cutting industry during 1.5 years of activity. *Microbiome* **9**, 204 (2021).
57. Young, C. C. W. et al. Antibiotic resistance genes of public health importance in livestock and humans in an informal urban community in Nepal. *Sci. Rep.* **12**, 13808 (2022).
58. EFSA Panel on Biological Hazards (BIOHAZ). et al. Role played by the environment in the emergence and spread of antimicrobial resistance (AMR) through the food chain. *EFSA J.* 19, e06651 (2021).
59. Li, D., Liu, C.-M., Luo, R., Sadakane, K. & Lam, T.-W. MEGAHIT: an ultra-fast single-node solution for large and complex metagenomics assembly via succinct de Bruijn graph. *Bioinformatics* **31**, 1674–1676 (2015).
60. Quijada, N. M., Rodríguez-Lázaro, D., Eiros, J. M. & Hernández, M. TORMES: an automated pipeline for whole bacterial genome analysis. *Bioinformatics* **35**, 4207–4212 (2019).
61. Wood, D. E., Lu, J. & Langmead, B. Improved metagenomic analysis with Kraken 2. *Genome Biol.* **20**, 257 (2019).
62. Hyatt, D. et al. Prodigal: prokaryotic gene recognition and translation initiation site identification. *BMC Bioinform.* **11**, 119 (2010).
63. Camacho, C. et al. BLAST+: architecture and applications. *BMC Bioinform.* **10**, 421 (2009).
64. Seemann, T. abricate. *GitHub* https://github.com/tseemann/abricate (2023).
65. Silamiķelis, I. Conifer. *GitHub* https://github.com/Ivarz/Conifer (2024).
66. Tamames, J. & Puente-Sánchez, F. Squeezemeta, a highly portable, fully automatic metagenomic analysis pipeline. *Front. Microbiol.* **9**, 3349 (2018).
67. Tange, O. Gnu Parallel 2018. *Zenodo* https://doi.org/10.5281/zenodo.1146014 (2018).
68. Schwengers, O. et al. Platon: identification and characterization of bacterial plasmid contigs in short-read draft assemblies exploiting protein sequence-based replicon distribution scores. *Microb. Genom.* **6**, mgen000398 (2020).
69. Camargo, A. P. et al. Identification of mobile genetic elements with geNomad. *Nat. Biotechnol.* **42**, 1303–1312 (2024).
70. Carattoli, A. et al. In silico detection and typing of plasmids using PlasmidFinder and plasmid multilocus sequence typing. *Antimicrob. Agents Chemother.* **58**, 3895–3903 (2014).
71. Néron, B. et al. IntegronFinder 2.0: identification and analysis of integrons across bacteria, with a focus on antibiotic resistance in *Klebsiella*. *Microorganisms* **10**, 700 (2022).
72. Cobo-Díaz, J. F. ARG-contig_mobilome_analysis. *GitHub* https://github.com/JoseCoboDiaz/ARG-contig_mobilome_analysis (2023).
73. Johansson, M. H. K. et al. Detection of mobile genetic elements associated with antibiotic resistance in *Salmonella enterica* using a newly developed web tool: MobileElementFinder. *J. Antimicrob. Chemother.* **76**, 101–109 (2021).
74. Groussin, M. et al. Elevated rates of horizontal gene transfer in the industrialized human microbiome. *Cell* **184**, 2053–2067 (2021).
75. Cantalapiedra, C. P., Hernández-Plaza, A., Letunic, I., Bork, P. & Huerta-Cepas, J. eggNOG-mapper v2: functional annotation, orthology assignments, and domain prediction at the metagenomic scale. *Mol. Biol. Evol.* **38**, 5825–5829 (2021).
76. Steinegger, M. & Söding, J. MMseqs2 enables sensitive protein sequence searching for the analysis of massive data sets. *Nat. Biotechnol.* **35**, 1026–1028 (2017).
77. Segata, N. MASTER-WP5-pipelines. *GitHub* https://github.com/SegataLab/MASTER-WP5-pipelines/blob/master/07-AMR_virulence_genes/emapper2gggenes.rb (2024).
78. Wilkins, D. gggenes: Draw Gene Arrow Maps in "ggplot2". R version 4.3.1 (2023).
79. NCBI Resource Coordinators. Database resources of the National Center for Biotechnology Information. *Nucleic Acids Res.* **42**, D7–D17 (2014).
80. Langmead, B. & Salzberg, S. L. Fast gapped-read alignment with Bowtie 2. *Nat. Methods* **9**, 357–359 (2012).
81. Kang, D. D. et al. MetaBAT 2: an adaptive binning algorithm for robust and efficient genome reconstruction from metagenome assemblies. *PeerJ* **7**, e7359 (2019).
82. Parks, D. H., Imelfort, M., Skennerton, C. T., Hugenholtz, P. & Tyson, G. W. CheckM: assessing the quality of microbial genomes recovered from isolates, single cells, and metagenomes. *Genome Res.* **25**, 1043–1055 (2015).
83. Pasolli, E. et al. Extensive unexplored human microbiome diversity revealed by over 150,000 genomes from metagenomes spanning age, geography, and lifestyle. *Cell* **176**, 649–662 (2019).
84. Ondov, B. D. et al. Mash: fast genome and metagenome distance estimation using MinHash. *Genome Biol.* **17**, 132 (2016).
85. Quijada, N. M. et al. FoodGenVir database. *Zenodo* https://doi.org/10.5281/zenodo.8344969 (2023).
86. R Core Team. R: A Language and Environment for Statistical Computing (R Foundation for Statistical Computing, 2023).
87. Gu, Z., Gu, L., Eils, R., Schlesner, M. & Brors, B. circlize implements and enhances circular visualization in R. *Bioinformatics* **30**, 2811–2812 (2014).
88. Gu, Z. Complex heatmap visualization. *iMeta* **1**, e43 (2022).
89. Wickham, H., François, R., Henry, L., Müller, K. & Vaughan, D. dplyr: A Grammar of Data Manipulation. R version 4.3.1 (2023).
90. Brunson, J. C. ggalluvial: layered grammar for alluvial plots. *J. Open Source Softw.* **5**, 2017 (2020).
91. Wickham, H. *ggplot2 – Elegant Graphics for Data Analysis* (Springer, 2016); https://doi.org/10.1007/978-0-387-98141-3
92. Yu, G., Smith, D. K., Zhu, H., Guan, Y. & Lam, T. T. Y. ggtree: an R package for visualization and annotation of phylogenetic trees with their covariates and other associated data. *Methods Ecol. Evol.* **8**, 28–36 (2016).

93. Frerebeau, N. nfrerebeau/khroma v1.3.0. *Zenodo* https://doi.org/10.5281/zenodo.1472077 (2019).
94. Kolde, R. pheatmap: Pretty Heatmaps. R version 4.3.1 (2019).
95. Wickham, H. Reshaping data with the reshape package. *J. Stat. Softw.* **21**, 1–20 (2007).
96. Wickham, H., Vaughan, D. & Girlich, M. tidyr: Tidy Messy Data. R version 4.3.1 (2023).

Acknowledgements

This work was funded by the European Commission under the European Union's Horizon 2020 research and innovation programme under grant agreement no. 818368 (MASTER). N.M.Q. is currently funded under the Generation D initiative, promoted by Red.es, an organization attached to the Ministry for Digital Transformation and the Civil Service, for the attraction and retention of talent through grants and training contracts, financed by the Recovery, Transformation and Resilience Plan through the European Union's Next Generation funds (ref. MMT24-IBFG-01). C.B. is grateful to Junta de Castilla y León and the European Social Fund for awarding her a predoctoral grant (grant no. BOCYL-D-07072020-6). The COMET-K1 competence centre FFoQSI (number 881882) is funded by the Austrian federal ministries BMK, BMDW and the Austrian provinces Lower Austria, Upper Austria and Vienna within the scope of COMET - Competence Centers for Excellent Technologies. The program COMET is handled by the Austrian Research Promotion Agency, FFG.

Author contributions

M.L., M.P., V.T.M., M.W., A.M., N.S., P.D.C., D.E. and A.A.-O. conceived the study and obtained the funding. N.M.Q., J.F.C.-D., V.V., C.B., F.D.F., R.C.-R., N.C., M.D., I.C.-T., C.S., L.R., S.K. and S.S. performed the samplings at food-processing facilities. N.M.Q., V.V., C.B., F.D.F., R.C.-R., N.C., M.D., I.C-T., C.S., S.K. and S.S. performed samples preprocessing and DNA extraction. F.P. and N.S. sequenced the extracted DNA. N.C. and F.P. performed the initial bioinformatic analyses, from raw reads to filtered reads, assembled contigs and binned MAGs. N.M.Q., J.F.C.-D., V.V., R.C.R., N.C. and C.S. collated all the metadata information. N.M.Q., J.F.C.-D. and V.V. performed the downstream bioinformagic and resistome analyses and prepared the figures. N.M.Q, J.F.C.-D., V.V. and A.A.-O. wrote the manuscript with input from all authors. All authors read and approved the final manuscript.

Competing interests

The authors declare no competing interests.

Additional information

Extended data is available for this paper at https://doi.org/10.1038/s41564-025-02059-8.

Supplementary information The online version contains supplementary material available at https://doi.org/10.1038/s41564-025-02059-8.

Correspondence and requests for materials should be addressed to Avelino Alvarez-Ordóñez.

Peer review information *Nature Microbiology* thanks Franck Carbonero and the other, anonymous, reviewer(s) for their contribution to the peer review of this work. Peer reviewer reports are available.

Reprints and permissions information is available at www.nature.com/reprints.

Publisher's note Springer Nature remains neutral with regard to jurisdictional claims in published maps and institutional affiliations.

[1]Austrian Competence Centre for Feed and Food Quality, Safety and Innovation, FFoQSI GmbH, Tulln an der Donau, Austria. [2]Clinical Department for Farm Animals and Food System Science, Centre for Food Science and Veterinary Public Health, University of Veterinary Medicine Vienna, Vienna, Austria. [3]Institute of Functional Biology and Genomics (IBFG), CSIC-USAL, Salamanca, Spain. [4]Department of Food Hygiene and Technology and Institute of Food Science and Technology, Universidad de León, Leon, Spain. [5]Department of Agricultural Sciences, University of Naples Federico II, Naples, Italy. [6]Task Force on Microbiome Studies, University of Naples Federico II, Naples, Italy. [7]Teagasc Food Research Centre, Cork, Ireland. [8]Institute of Agrochemistry and Food Technology, National Research Council (IATA-CSIC), Paterna, Spain. [9]Department of Cellular, Computational and Integrative Biology, University of Trento, Trento, Italy. [10]Dairy Research Institute of Asturias, Spanish National Research Council (IPLA-CSIC), Oviedo, Spain. [11]Health Research Institute of Asturias (ISPA), Avenida Hospital Universitario, Oviedo, Spain. [12]Queen's University Belfast, Belfast, UK. [13]Consiglio Nazionale delle Ricerche, Bari, Italy. [14]Microbiology Research Group, Matís Ltd, Reykjavik, Iceland. [15]Faculty of Food Science and Nutrition, University of Iceland, Reykjavik, Iceland. [16]APC Microbiome Ireland and VistaMilk Research Centres, Cork, Ireland. [17]These authors contributed equally: Narciso M. Quijada, José F. Cobo-Díaz, Vincenzo Valentino. ✉e-mail: aalvo@unileon.es

https://doi.org/10.1038/s41564-025-02059-8

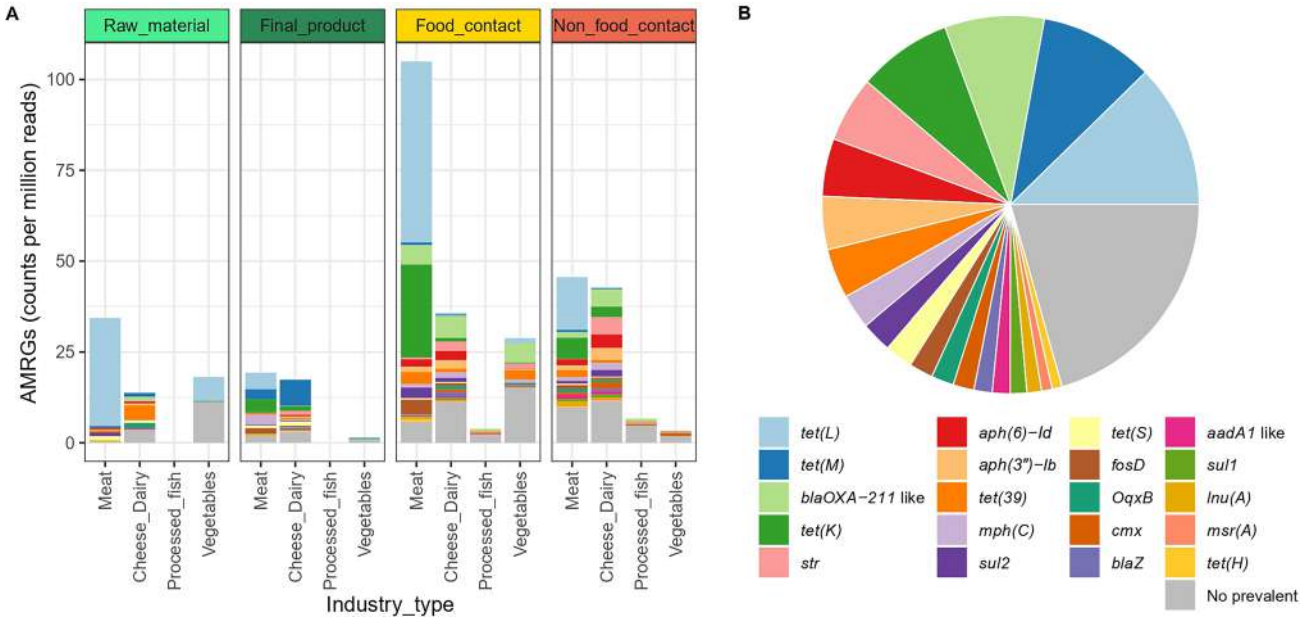

Extended Data Fig. 1 | Main prevalent AMRG. Mean values of prevalent AMRG (> 0.1 CPM in >10% samples) found **a**) by sample type and industry type and **b**) percentage of prevalent AMRG found globally.

https://doi.org/10.1038/s41564-025-02059-8

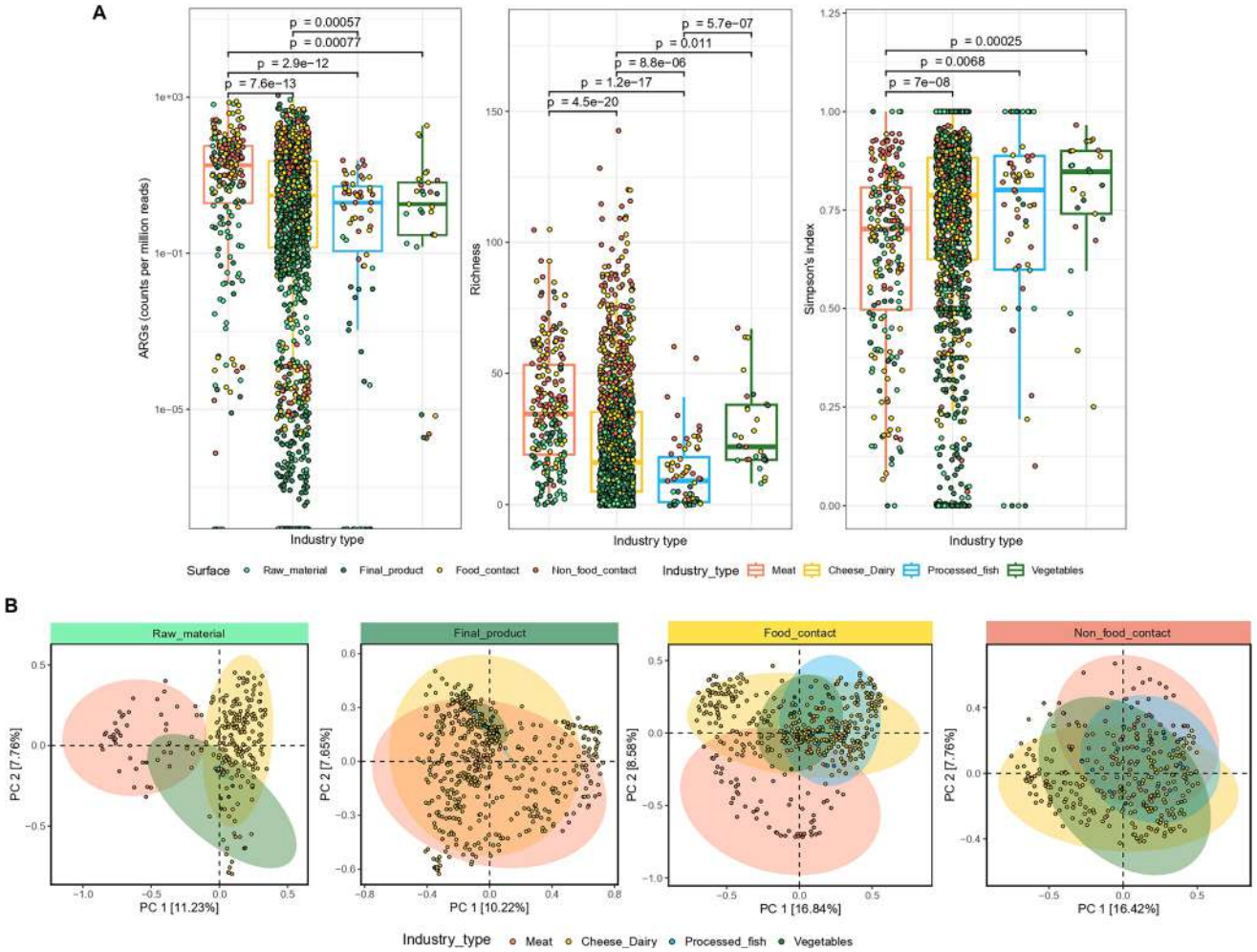

Extended Data Fig. 2 | Quantitative overview of AMRG occurrence in foods and food processing environments. a) Total AMRG counts, richness index and Simpson's evenness index for AMRG. **b**) Principal Coordinates Analysis for AMRG counts normalised to CPM.

https://doi.org/10.1038/s41564-025-02059-8

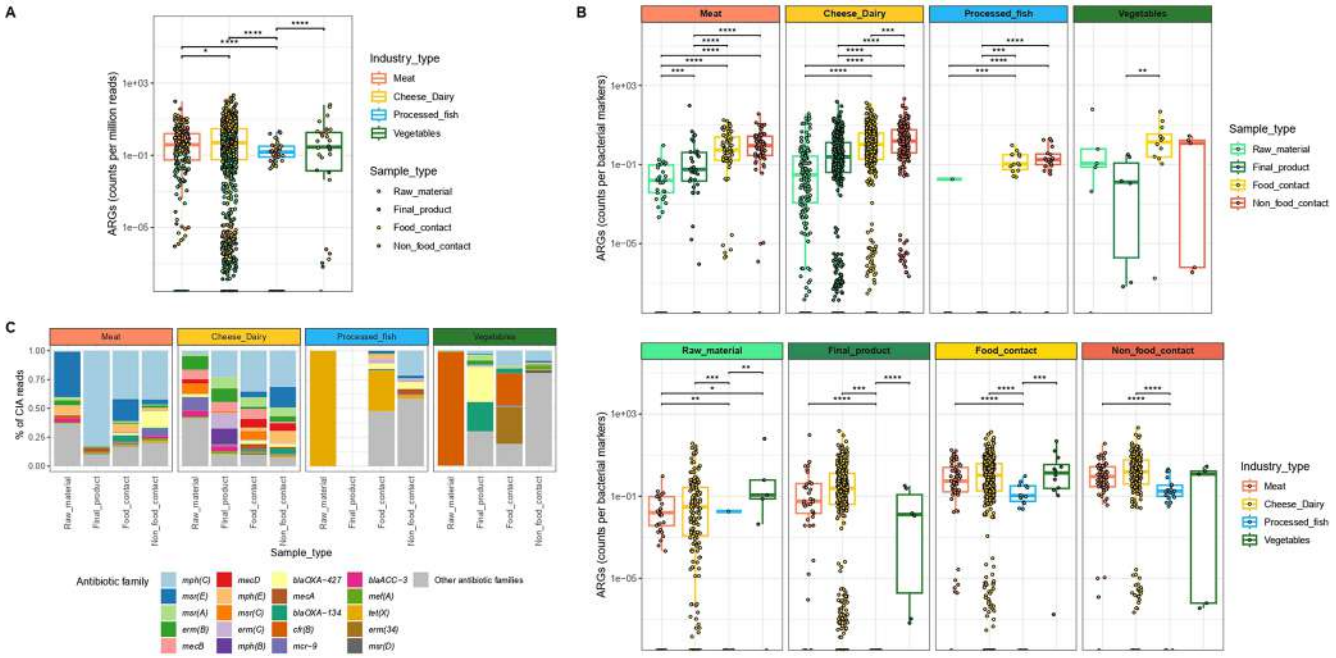

Extended Data Fig. 3 | Quantitative overview of CIA AMRG occurrence in foods and food processing environments. a) Global CIA AMRG abundance as CPM. **b**) Differences in CIA AMRG counts among sample types from the same industry type (top boxplot) and among industry types for the same sample type (bottom boxplot). **c**) Relative abundance of the 20 most abundant CIA AMRG.

https://doi.org/10.1038/s41564-025-02059-8

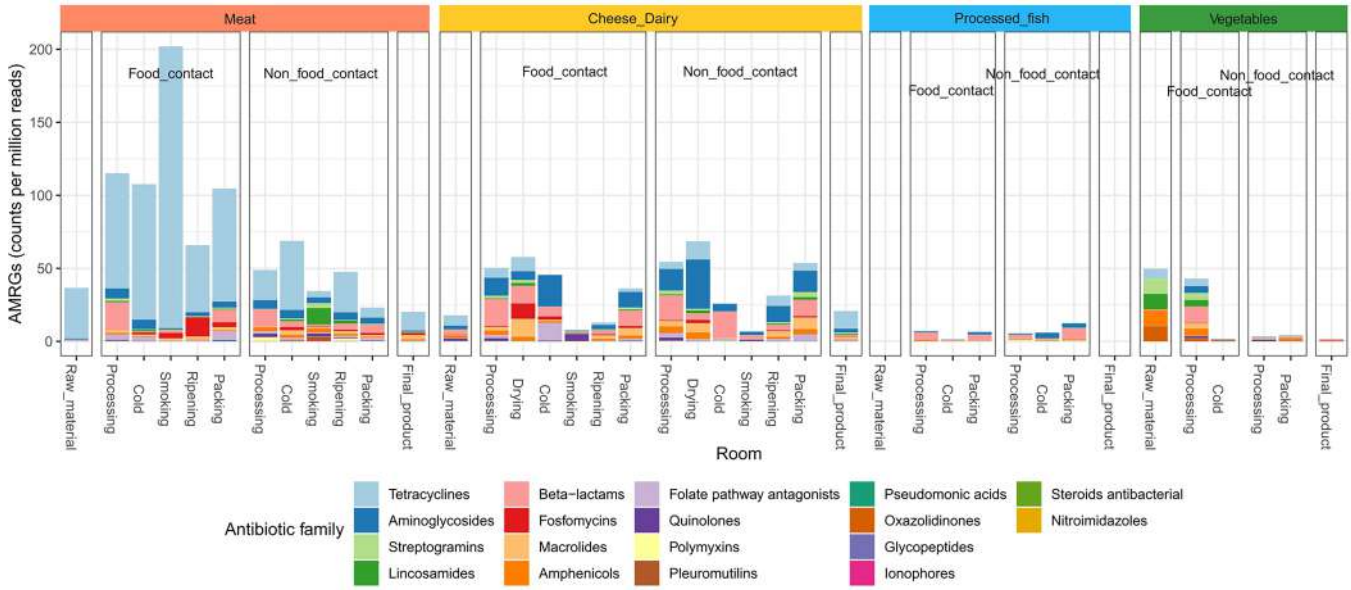

Extended Data Fig. 4 | Antibiotic families distribution along different rooms. For both FC and NFC samples in each industry type studied.

https://doi.org/10.1038/s41564-025-02059-8

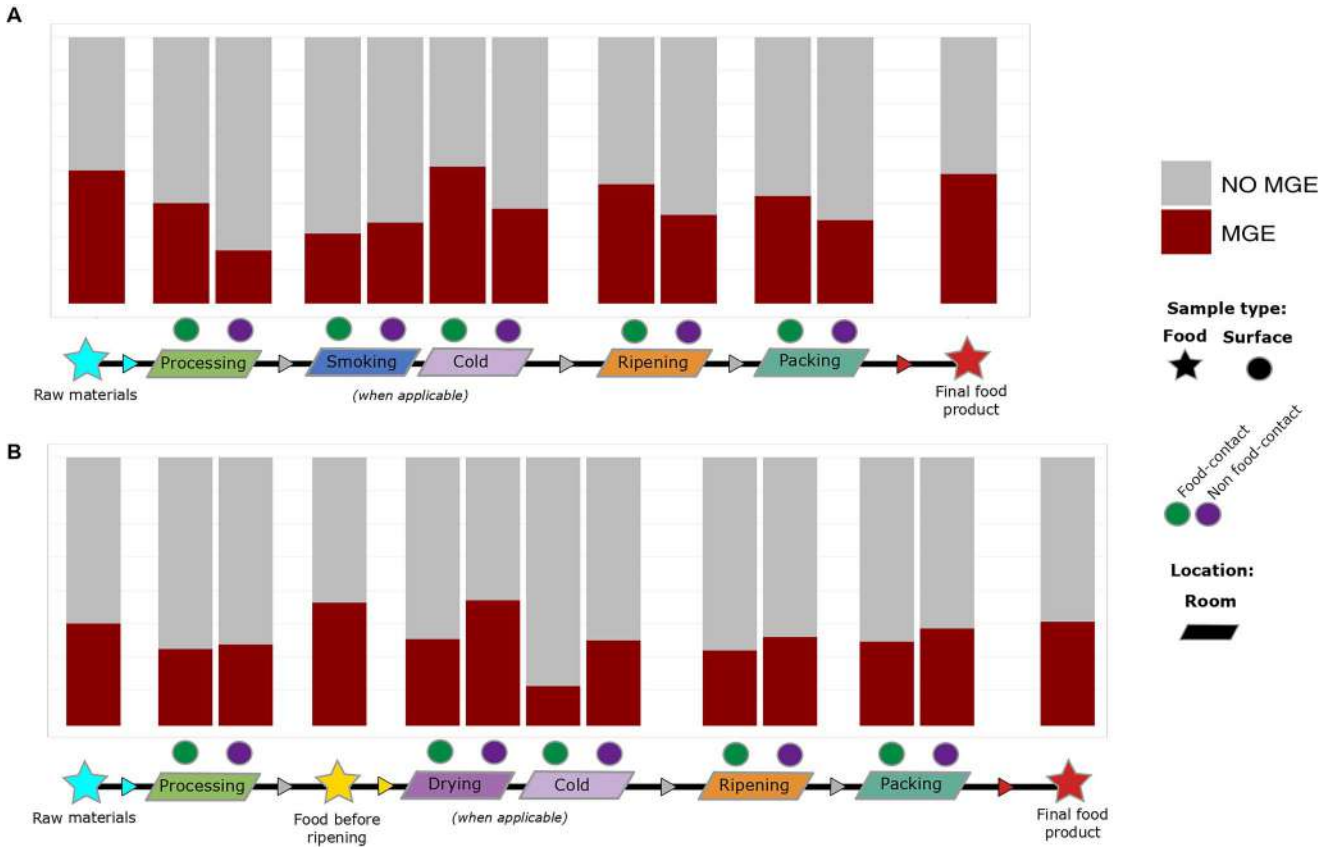

Extended Data Fig. 5 | Ratio of AMRG-carrying contigs. Association with MGE in the different surfaces and rooms in meat (**a**) and dairy (**b**) industry.

https://doi.org/10.1038/s41564-025-02059-8

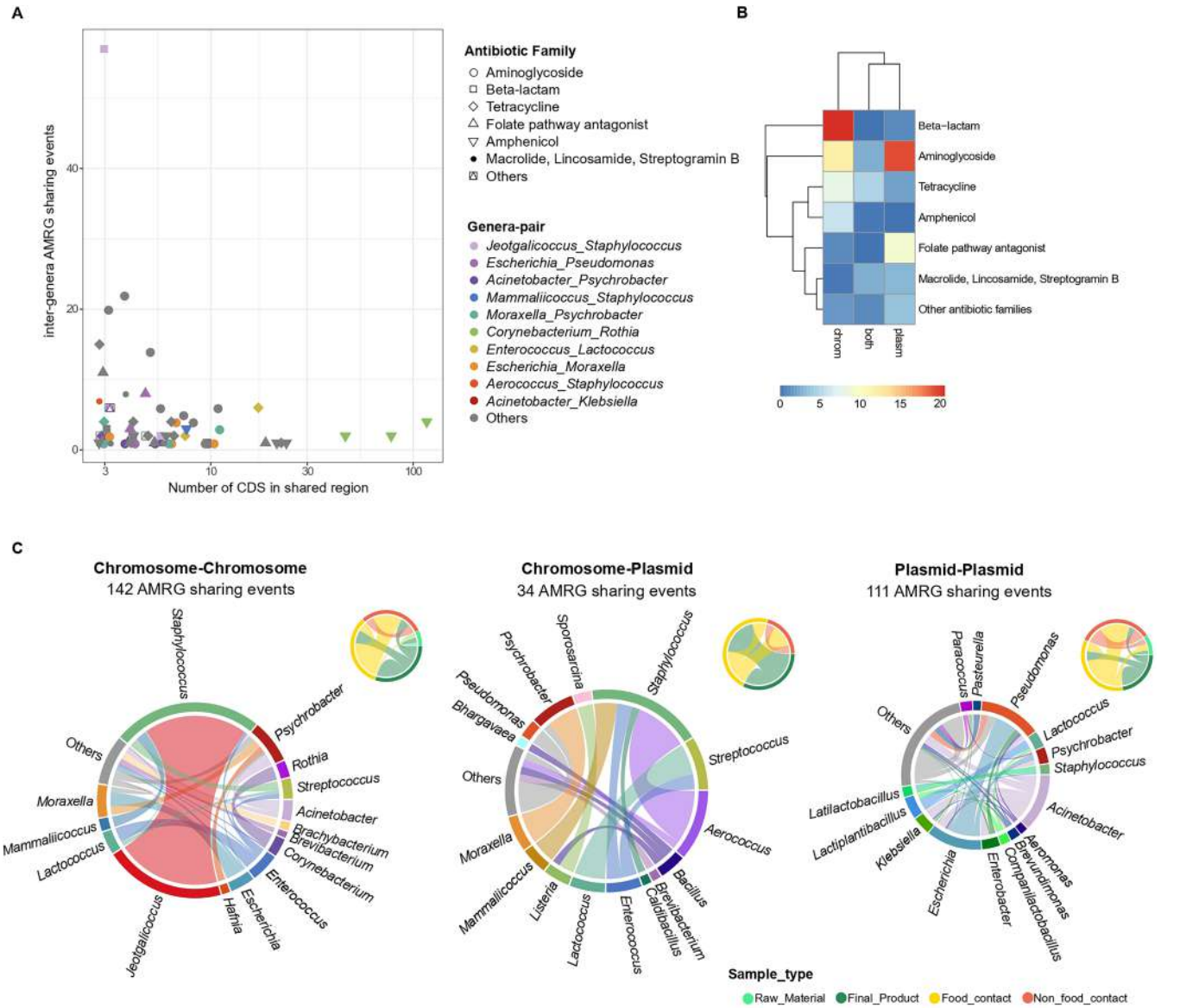

Extended Data Fig. 6 | Inter-genera AMRG sharing events detected. a) Number of AMRG sharing events found and number of CDS within each AMRG sharing region. The point shape indicates AM class and the color indicates the genera-pair involved in the AMRG sharing events. **b**) AMRG sharing events (genera-pair) detected between chromosomes, chromosomes-plasmids and plasmids. **c**) AMRG sharing events abundance according to plasmidic (plasm), chromosomic (chrom) or hybrid (both) gene interchange. Small chord diagrams indicated AMRG shared events between sample type.

https://doi.org/10.1038/s41564-025-02059-8

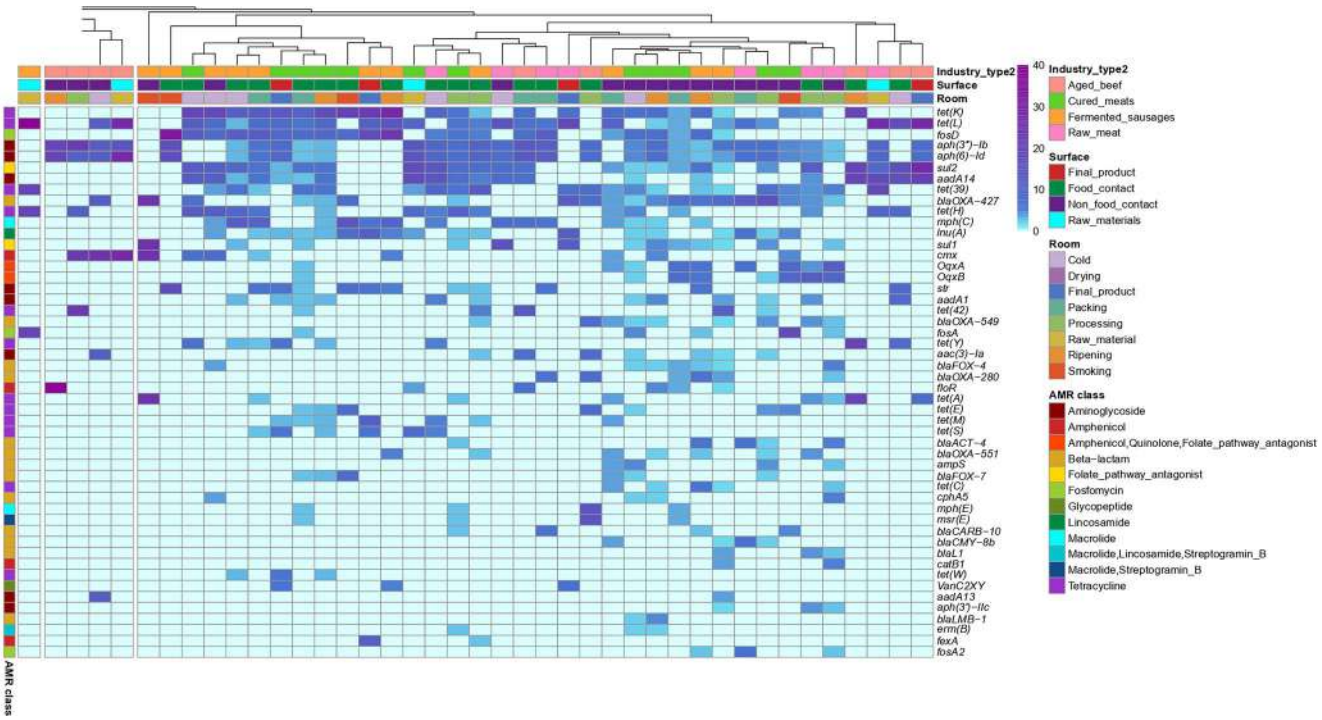

Extended Data Fig. 7 | AMRG-carrier species distribution along meat production surfaces and relationship with their resistome profile. Relative abundance of the 50 most abundant AMRG in meat facilities. The type of meat product elaborated in each facility is indicated as "Industry_type2". The AM class of each gene is colour-indicated on the left part, while sample type and facility room are colour-indicated on top. The heatmap colour scale indicates the number of AMRG identified for each surface.

https://doi.org/10.1038/s41564-025-02059-8

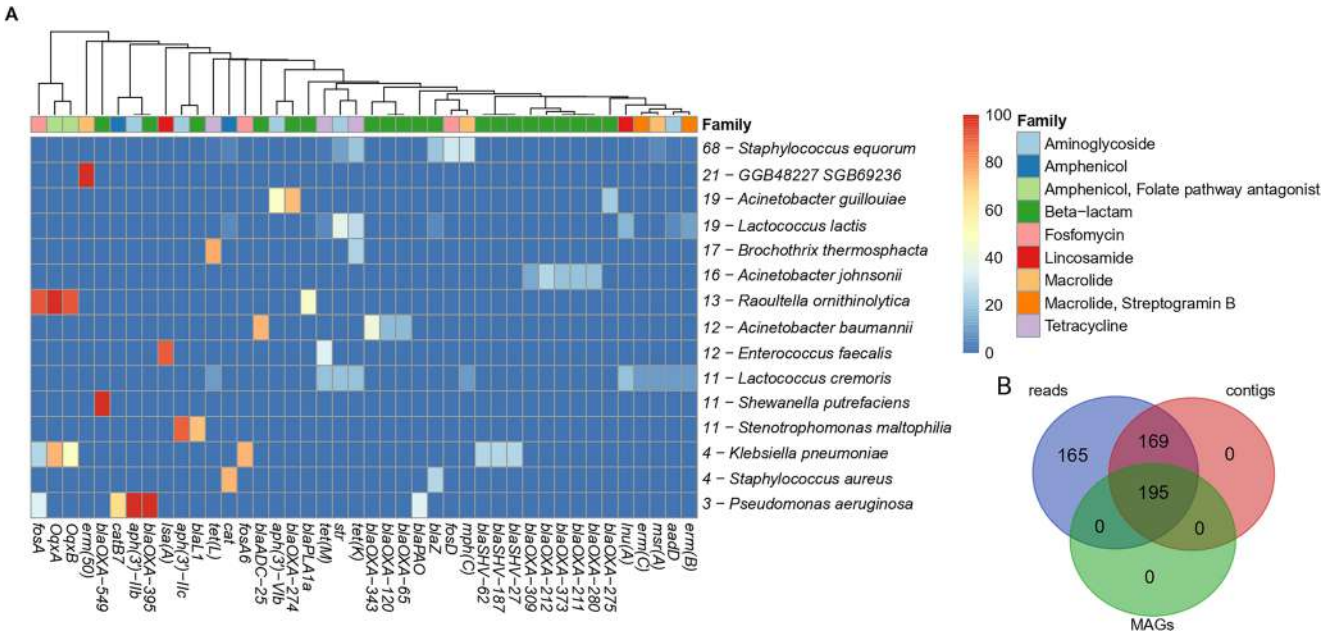

Extended Data Fig. 8 | Analysis of AMRG-carrying MAGs. a) Percentage of MAGs obtained per each species (y-axis) that carried the most abundant AMRG (x-axis). Only species with more than 10 AMRG-carrying MAGs were represented (K. pneumoniae, S. aureus and P. aeruginosa were also represented to cover the ESKAPEE group). The number written before each species name indicates the number of AMRG-carrying MAGs found for each species. **b**) Venn diagram comparing the number of AMRG-clusters found when assessing the resistome using the reads, the contigs or the MAGs datasets.

nature portfolio

Corresponding author(s): Avelino Álvarez-Ordóñez

Last updated by author(s): May 22, 2025

Reporting Summary

Nature Portfolio wishes to improve the reproducibility of the work that we publish. This form provides structure for consistency and transparency in reporting. For further information on Nature Portfolio policies, see our Editorial Policies and the Editorial Policy Checklist.

Statistics

For all statistical analyses, confirm that the following items are present in the figure legend, table legend, main text, or Methods section.

n/a	Confirmed	
☐	☒	The exact sample size (*n*) for each experimental group/condition, given as a discrete number and unit of measurement
☐	☒	A statement on whether measurements were taken from distinct samples or whether the same sample was measured repeatedly
☐	☒	The statistical test(s) used AND whether they are one- or two-sided *Only common tests should be described solely by name; describe more complex techniques in the Methods section.*
☒	☐	A description of all covariates tested
☐	☒	A description of any assumptions or corrections, such as tests of normality and adjustment for multiple comparisons
☐	☒	A full description of the statistical parameters including central tendency (e.g. means) or other basic estimates (e.g. regression coefficient) AND variation (e.g. standard deviation) or associated estimates of uncertainty (e.g. confidence intervals)
☐	☒	For null hypothesis testing, the test statistic (e.g. *F*, *t*, *r*) with confidence intervals, effect sizes, degrees of freedom and *P* value noted *Give P values as exact values whenever suitable.*
☒	☐	For Bayesian analysis, information on the choice of priors and Markov chain Monte Carlo settings
☒	☐	For hierarchical and complex designs, identification of the appropriate level for tests and full reporting of outcomes
☒	☐	Estimates of effect sizes (e.g. Cohen's *d*, Pearson's *r*), indicating how they were calculated

Our web collection on statistics for biologists contains articles on many of the points above.

Software and code

Policy information about availability of computer code

Data collection	No software was used for data collection.
Data analysis	The software used is thoroughly described in the "Materials and Methods" section and available in the public repositories https://github.com/nmquijada/MASTER-food-production-resistome, https://github.com/SegataLab/cFMD and https://github.com/SegataLab/MASTER-WP5-pipelines. List of software used: TrimGalore v0.6.7, ViromeQC v1.0.2, CD-HIT v4.8.1, MEGAHIT v1.2.9, TORMES v1.3.0, GNU-Parallel v20201122, kraken2 v2.0.8, Prodigal v2.6.3, BLASTN v2.9.0+, ABRicate v1.0.1, Platon v1.6, geNomad v1.6.1, IntegronFinder v2.0.1, WAAFLE v1.0.0, MobileElementFinder v1.0.5, eggnog-mapper v2.1.11, MMseqs2 v13.45111, bowtie2 v2.2.9, MetaBAT v2.12.1, CheckM v1.0.13. R environment v4.3.1 and packages: circlize v0.4.16, ComplexHeatmap v2.22.0, dplyr v1.1.4, ggalluvial v0,12.5, gggenes v0.5.1, ggplot2 v3.5.1, ggpubr v0.6.0, ggtree v3.14.0, khroma v1.16.0, pheatmap v1.0.12, reshape2 v1.4.4, tidyr v1.3.1 and vegan v2.6.10.

For manuscripts utilizing custom algorithms or software that are central to the research but not yet described in published literature, software must be made available to editors and reviewers. We strongly encourage code deposition in a community repository (e.g. GitHub). See the Nature Portfolio guidelines for submitting code & software for further information.

Data

Policy information about availability of data

All manuscripts must include a data availability statement. This statement should provide the following information, where applicable:

- Accession codes, unique identifiers, or web links for publicly available datasets
- A description of any restrictions on data availability
- For clinical datasets or third party data, please ensure that the statement adheres to our policy

The raw sequencing data collected in the study is publicly available on the Sequence Read Archive of the National Center of Biotechnology (BioProject numbers PRJNA897099, PRJNA997800 and PRJNA997821) and on the European Nucleotide Archive (accession numbers PRJEB62794 and PRJEB63604), as stated in the the "Data availability" section of "Materials and Methods". The specific BioSampleID, BioProject and accession codes for each sample, together with further metadata is provided in Supplementary Table 5. FoodGenVir database is publicly accessible at https://doi.org/10.5281/zenodo.8344969

Research involving human participants, their data, or biological material

Policy information about studies with human participants or human data. See also policy information about sex, gender (identity/presentation), and sexual orientation and race, ethnicity and racism.

Reporting on sex and gender	Not applicable
Reporting on race, ethnicity, or other socially relevant groupings	Not applicable
Population characteristics	Not applicable
Recruitment	Not applicable
Ethics oversight	Not applicable

Note that full information on the approval of the study protocol must also be provided in the manuscript.

Field-specific reporting

Please select the one below that is the best fit for your research. If you are not sure, read the appropriate sections before making your selection.

☒ Life sciences ☐ Behavioural & social sciences ☐ Ecological, evolutionary & environmental sciences

For a reference copy of the document with all sections, see nature.com/documents/nr-reporting-summary-flat.pdf

Life sciences study design

All studies must disclose on these points even when the disclosure is negative.

Sample size	An in-depth SOP for food-industry sampling was carefully designed and discussed among all authors and published in Nature Communications (Barcenilla et al., 2024). For the study, we collected a total of 1,780 samples from 113 food industries and include 824 from processing environments, 254 from raw materials and 702 final product samples. Full information regarding each sample is provided in Extended Data Table 2
Data exclusions	No samples were discarded for the analyses
Replication	Due to the nature of the samples collected that belonged to food production batches that were followed through time, replication was not performed
Randomization	Randomization was considered in: - Sample collection: the specific raw materials, foods, and surfaces were selected during sampling visits from sample categories previously established, randomly collected by each individual in the day of sampling based on their availability (i.e. floor, walls, shelves, tables, knifes, etc.) and pooled (e.g. 5 swabs from FCS/NFCS samples were combined into a single pool for DNA extraction and sequencing). The sampling protocol was carefully examinized and decission points were compared and discussed thoroughly in Barcenilla et al., Nature Protocols, 2024, doi: https://doi.org/10.1038/s41596-023-00949-x. - DNA extraction: while randomization for sample pre-processing was not possible (i.e., different sample categories require different pre-processing, each industry had to be pre-processed individually on the sampling day), samples were randomised for DNA extraction. - Bioinformatic analysis: an automated standardized pipeline was followed to ensure blind processing. Initial exploratory analyses were performed without linking samples to groups.
Blinding	Samples were labeled with codes so that lab technicians processing DNA and preparing sequencing libraries did not know their group origin. For bioinformatic analyses, an automated standardized pipeline was followed to ensure blind processing. Moreover, initial exploratory analyses were performed without linking samples to groups.

Reporting for specific materials, systems and methods

We require information from authors about some types of materials, experimental systems and methods used in many studies. Here, indicate whether each material, system or method listed is relevant to your study. If you are not sure if a list item applies to your research, read the appropriate section before selecting a response.

Materials & experimental systems

n/a	Involved in the study
☒	☐ Antibodies
☒	☐ Eukaryotic cell lines
☒	☐ Palaeontology and archaeology
☒	☐ Animals and other organisms
☒	☐ Clinical data
☒	☐ Dual use research of concern
☒	☐ Plants

Methods

n/a	Involved in the study
☒	☐ ChIP-seq
☒	☐ Flow cytometry
☒	☐ MRI-based neuroimaging

Plants

Seed stocks	Not applicable
Novel plant genotypes	Not applicable
Authentication	Not applicable